Flavour-changing Higgs decays into bottom and strange quarks in supersymmetry

G. Barenboim,[1, *] C. Bosch,[1, †] J.S. Lee,[2, ‡] M.L. López-Ibáñez,[1, §] and O. Vives[1, ¶]

[1]*Departament de Física Teòrica and IFIC,*

Universitat de València-CSIC, E-46100, Burjassot, Spain.

[2]*Department of Physics, Chonnam National University,*

300 Yongbong-dong, Buk-gu, Gwangju, 500-757, Republic of Korea

In this work, we explore the flavour changing decays $H_i \to bs$ in a general supersymmetric scenario. In these models, the flavour changing decays arise at loop-level but, originating from a dimension-four operator, do not decouple and may provide a first sign of new physics for heavy masses beyond collider reach. In the framework of the minimal supersymmetric extension of the Standard Model (MSSM), we find that the largest branching ratio of the lightest Higgs (H_1) is $\mathcal{O}(10^{-6})$ after imposing present experimental constraints, while heavy Higgs states may still present branching ratios $\mathcal{O}(10^{-3})$. In a more general supersymmetric scenario, where additional Higgs states may modify the Higgs mixings, the branching ratio $\mathrm{BR}(H_1 \to bs)$ can reach values $\mathcal{O}(10^{-4})$, while heavy Higgses still remain at $\mathcal{O}(10^{-3})$. Although these values are clearly out of reach for the LHC, a full study in a linear collider environment could be worth.

---

*Electronic address: Gabriela.Barenboim@uv.es

†Electronic address: Cristian.Bosch@uv.es

‡Electronic address: jslee@jnu.ac.kr

§Electronic address: M.Luisa.Lopez-Ibanez@uv.es

¶Electronic address: Oscar.Vives@uv.es

I.   INTRODUCTION

Since the discovery of a scalar boson with mass $\sim$126 GeV, at the LHC in 2012 [1, 2], the Standard Model (SM) picture may have been completed. Indeed, if this scalar particle corresponds to the SM Higgs boson, the SM could be the correct description of nature up to scales close to the Planck mass. So far, all the experimental evidence seems to be pointing in the direction of confirming that it is really the missing piece of the SM puzzle. Nevertheless the exploration of features of this particle is just beginning and further studies are needed to confirm its identity.

From now on, our efforts to probe the SM and to search for physics beyond it may follow two complementary paths: i) push the energy frontier in the search for new particles and interactions and ii) increase the precision on the couplings of the first (so far) fundamental scalar ever discovered. Indirect searches, which would include the latter path, searches of rare processes or higher order corrections to low energy couplings, have been very successful in the past and have led to the discovery of new particles such as the third generation quarks. They have also been instrumental in exploring the scale of new physics beyond the collider reach.

In the case of the Higgs boson, the study of its couplings can be the way to go. Scrutinizing non-standard Higgs couplings is a way to test the presence of additional scalar bosons even when their direct production is closed. In the models beyond the SM in which there exists more than one Higgs doublet, as in a two Higgs doublet model (2HDM)[3] or the MSSM [4, 5], the couplings of the candidate for the discovered scalar boson may not be flavour diagonal and thus it can have flavour changing decays [6–23]. Furthermore, these flavour changing couplings are dimensionless and therefore the effects of additional heavy particles may not decouple even when the masses of such particles are taken to infinity, providing a unique opportunity to find an assuring indirect evidence for such a high scale non-easily accessible in the near future.

Even more, as we have no clue of the new energy scale (if any) associated with the new particles and interactions we are looking for, considering rare Higgs decays is a wise way to go. Thus, our proposal consists of searching for the Flavour-Changing (FC) Higgs decays. In the SM these FC decays do not exist and therefore their presence would undoubtedly signal the presence of new physics beyond the SM.

As mentioned before, in the past, rare decays, including processes like $b \to s\,\gamma$ and $B_s \to \mu^+\,\mu^-$, have been extensively used to search for new physics. Their precise experimental measurements were useful for the exploration of the parameter space of different SM extensions. Likewise, FC Higgs decays are very useful to search for new physics since they are present in almost any extension

of the SM containing additional scalars that mix with the lighter Higgs. For instance they are unavoidable in type-II 2HDMs, like the MSSM, pseudo-dilaton models [24, 25], models with extra dimensions [26, 27] or composite Higgs models [28]. To be specific, in this work we will explore a generic supersymmetric scenario, as well as the MSSM framework, both in the presence of non-minimal flavour structures.

Our analysis will be focused on the process $H \to b\,s$, since one would expect on general grounds that, among FC Higgs decays, those involving third generation particles whose Yukawa couplings are larger are the most experimentally accessible. Besides, loop-induced FC processes in the quark sector are typically larger by a factor α_3^2/α_2^2 (where α_3 and α_2 are the coupling constants associated to the groups $SU(3)$ and $SU(2)$ respectively) for similar flavour changing entries in the lepton sector.

The main goal in this analysis is to find out the largest FC branching ratios for the different Higgs states attainable in a general supersymmetric scenario. As we will show, in the MSSM, the decoupling of the heavy Higgses, enforced by present constraints, makes the FC branching ratio (BR) of the observed light-Higgs to be below the level of 10^{-6}, while heavy Higgs states could reach $\sim 10^{-3}$. In a more general supersymmetric standard model, the light Higgs BR could still reach values of $\sim 10^{-4}$. Thus, these rare decays are very challenging for the LHC but they can be searched for at lepton colliders as the International Linear Collider (ILC). As will be shown, the branching ratio can reach a level of 10^{-3} under special circumstances in the generic SUSY case. These branching ratios could be reached at a linear collider. In fact, we can see that already at LEP, a limit of $\mathrm{BR}(Z \to b\bar{s}) < O(10^{-3})$ was obtained with only $O(10^6)$ Z-bosons in Ref. [29]. We can expect the larger statistics and improved experimental techniques to improve these limits (see also [30]). In the case of the Higgs decays, we can produce between $O(10^5)$ and $O(10^6)$ Higgs bosons for $m_H = 125$ GeV [31], and therefore we can expect similar values for the lightest Higgs branching ratio. Thus, FC Higgs decays may provide an indirect hint for the existence of new physics at higher energies even when these higher scales are beyond the LHC or ILC reach.

This paper is organized as follows: in section II, we introduce the framework in which the analysis will be carried out. Some compelling variations of it will also be addressed because of their interest when trying to observe FC processes. Still in this section, the theoretical expressions for the FC Higgs decays into down-type quarks will be provided. Section III summarizes the latest experimental data corresponding to collider probes and indirect bounds from low-energy experiments. Finally, section IV collects the main features of the numerical analysis, concluding in section V with the main results.

II.   HIGGS FLAVOUR CHANGING IN THE MSSM

Our analysis is performed within a generic CP-violating MSSM framework and its extensions, in which the minimal Higgs sector is a type-II 2HDM, *i.e.* one of the two scalar doublets couples only to the up-type quarks at tree-level while the other couples only to down-type quarks. When electroweak symmetry breaking (EWSB) occurs, the neutral components of the two Higgs fields acquire vacuum expectation values (VEVs) and five physical Higgs states appear: three with neutral electric charge and two charged bosons. The two Higgs doublets can be parameterized as

$$\Phi_1 \; = \; \begin{pmatrix} \Phi_1^0 \\ \phi_1^- \end{pmatrix}, \qquad \Phi_2 \; = \; e^{i\xi} \begin{pmatrix} \phi_2^+ \\ \Phi_2^0 \end{pmatrix} \tag{1}$$

where $\Phi_i^0 \; = \; \frac{1}{\sqrt{2}} \left(v_i + \phi_i + i\, a_i \right)$, with $v_1 = v \cos\beta$, $v_2 = v \sin\beta$ and $v \simeq 246$ GeV. At tree level the mass eigenstates (H_i) are CP eigenstates, but this situation changes once loop corrections are taken into account [32–38]. In the MSSM, the possibility of having CP-violating phases increases due to the growing number of complex parameters in the so-called soft SUSY breaking terms, and indeed these CP phases contribute at loop-level to Higgs masses and mixings. Consequently, weak-state fields ($\phi_{1,2}$ and a) give rise to CP-mixed mass eigenstates (H_i) and these states are related through a unitary transformation represented by the 3×3 orthogonal mixing matrix $\mathcal{O}$:

$$\phi_1 \; = \; \mathcal{O}_{1i}\, H_i, \qquad \phi_2 \; = \; \mathcal{O}_{2i}\, H_i, \qquad a \; = \; \mathcal{O}_{3i}\, H_i. \tag{2}$$

The mass eigenvalues will be obtained by means of diagonalising the mass squared matrix:

$$\mathcal{O}^T \cdot \mathcal{M}_H^2 \cdot \mathcal{O} \; = \; \mathrm{Diag}\left(m_{H_1}^2, m_{H_2}^2, m_{H_3}^2 \right) \tag{3}$$

To study Higgs flavour changing decays, it is helpful to introduce a convenient parametrization of the Higgs mixings. During the analysis, we will use

$$\delta_1 \; \equiv \; \left(\frac{\mathcal{O}_{11}}{\cos\beta} - \frac{\mathcal{O}_{21}}{\sin\beta} \right) \qquad \eta_1 \; \equiv \; \frac{\mathcal{O}_{31}}{\sin\beta \cos\beta}, \tag{4}$$

where δ_1 quantifies the distance of the lightest Higgs mixings from $\cos\beta$ and $\sin\beta$ and η_1 is directly related to the pseudoscalar content of H_1.

In our analysis below, we will distinguish two different situations in regard to the Higgs mixing:

- Full MSSM framework: Here, we consider the usual MSSM Higgs potential [5] which breaks the electroweak symmetry radiatively. The minimization of this potential gives us the Higgs masses and mixings.

Using $\mathcal{O}_{11}^2 + \mathcal{O}_{21}^2 + \mathcal{O}_{31}^2 = 1$, one may express the mixing angles $\mathcal{O}_{\alpha 1}$ in terms of δ_1 and η_1 as follows

$$
\begin{aligned}
\mathcal{O}_{11} &= \cos\beta \left[\sqrt{1 - (\delta_1^2 + \eta_1^2)\cos^2\beta\sin^2\beta} + \delta_1 \sin^2\beta \right], \\
\mathcal{O}_{21} &= \sin\beta \left[\sqrt{1 - (\delta_1^2 + \eta_1^2)\cos^2\beta\sin^2\beta} - \delta_1 \cos^2\beta \right], \\
\mathcal{O}_{31} &= \eta_1 \cos\beta \sin\beta .
\end{aligned}
\tag{5}
$$

Then, the coupling of the lightest Higgs to a pair of massive vector bosons is given by

$$
g_{H_1 VV} = \cos\beta\, \mathcal{O}_{11} + \sin\beta\, \mathcal{O}_{21} = \sqrt{1 - (\delta_1^2 + \eta_1^2)\cos^2\beta\sin^2\beta} .
\tag{6}
$$

The current LHC Higgs data constrain $g_{H_1 VV}$ to be close to its SM value, $g_{H_1 VV} = 1$. In fact, the present best-fit values and uncertainties are $\kappa_V = g_{H_1 VV} = 1.15 \pm 0.08$ if we assume there is no change in the Higgs total width, *i.e.* $\kappa_H^2 = \Gamma_H / \Gamma_H^{\mathrm{SM}} = 1$, and $\kappa_{VV} = \kappa_V \cdot \kappa_V / \kappa_H = 1.28^{+0.16}_{-0.15}$ if we allow for a change in the total decay width [39]. At present, the errors are still large, but requiring, for example, $g_{H_1 VV} \gtrsim 0.9$, one needs to have $(\delta_1^2 + \eta_1^2)\cos^2\beta\sin^2\beta \lesssim 0.2$. As we will show later, $\mathrm{BR}\left(H_1 \to \bar{b}s + \bar{s}b\right)$ is directly proportional to the quantity $(\delta_1^2 + \eta_1^2)$ which can be larger for larger $\tan\beta$ values while satisfying this constraint. On the other hand, large $\tan\beta$ values are constrained by the $\Delta B = 1$ and $\Delta B = 2$ processes such as $b \to s\gamma$, $B_s^0 \to \mu^+\mu^-$, $B_s^0 - \bar{B}_s^0$ mixing, etc. Taking into account all these constraint, we find that, $\mathrm{BR}\left(H_1 \to \bar{b}s + \bar{s}b\right)$ can be as large as 10^{-6} in an MSSM framework.

- Generic supersymmetric SM: Given that no signs of supersymmetry have been found so far in collider experiments, and taking into account the strong constraints on the parameter space of minimal models, it is interesting to consider more general models. In fact, the situation could be different if we consider SUSY models beyond the MSSM which contain additional Higgs states. In this case, the Higgs mass eigenstates H_i are given by

$$
H_i = \sum_{\alpha = 1,2} \mathcal{O}_{\alpha i}\, \phi_\alpha + \mathcal{O}_{3i}\, a + \sum_{\beta \geq 4} \mathcal{O}_{\beta i}\, \varphi_\beta
\tag{7}
$$

where φ_β represent the additional CP-even and CP-odd Higgs states which can be charged or neutral under $SU(2)_L$. We note that only the $SU(2)_L$-charged CP-even states contribute to the tree-level $g_{H_i VV}$ couplings and, due to the additional states, we generically have $\mathcal{O}_{11}^2 + \mathcal{O}_{21}^2 + \mathcal{O}_{31}^2 < 1$. As in the MSSM framework, these couplings are constrained by the experimental results on Higgs decays, but in the presence of other Higgs states close to the 125-GeV state, the mixing pattern could be different from that in the MSSM and δ_1 and/or

η_1 can be sizeable. In this case, one may treat δ_1 and η_1 as free parameters effectively. We find that, in this case, BR $\left(H_1 \to \bar{b}s + \bar{s}b\right)$ can be as large as 10^{-4}.

Processes mediated by flavor changing neutral currents (FCNCs) involving down-type quarks have been largely studied in the context of 2HDM where significant contributions can be accommodated due to the $\tan\beta$-enhancement of their Yukawa couplings. This type of processes are very useful for investigating the dynamics of quark-flavour mixing, especially the possible non-standard phenomena. Here, our main purpose is studying transitions such as $H_i \to bs$, keeping always under control other processes that will impose additional experimental constraints, for instance, the B-meson decay $B_s \to \mu^+\mu^-$ and the mass difference ΔM_{B_s} [1].

A. FC couplings

It is well-known that, in the MSSM, the superpotential holomorphicity prevents the appearance of Higgs-boson FCNCs by coupling the Higgs-doublet superfield Φ_1 to the down-quark sector and Φ_2 to the up-quark sector. However, this property is violated when considering finite radiative (threshold) corrections due to soft SUSY-breaking interactions [42–54]. As a consequence, Higgs-mediated FCNCs show up at the one-loop level. The general effective Yukawa Lagrangian for down-type quarks may be simply written as [55]:

$$-\mathcal{L}_Y^d = \bar{d}_R^0 \, \mathbf{h_d} \left[\left(\mathbf{1} + \boldsymbol{\Delta}_d^{\phi_1}\right) \frac{v_1 + \phi_1}{\sqrt{2}} - i \left(\mathbf{1} + \boldsymbol{\Delta}_d^{a_1}\right) \frac{a_1}{\sqrt{2}}\right] d_L^0 + \bar{d}_R^0 \, \mathbf{h_d} \left[\boldsymbol{\Delta}_d^{\phi_2} \frac{v_2 + \phi_2}{\sqrt{2}} - i \, \boldsymbol{\Delta}_d^{a_2} \frac{a_2}{\sqrt{2}}\right] d_L^0 + \text{H.c.}$$
(8)

where $\mathbf{h_d}$ is the tree-level Yukawa matrix and $d_{L,R}^0$ refer to the weak eigenstates. After EWSB, this Lagrangian gives rise to the d-quarks mass terms and also to the Higgs-mediated FC terms. For the former, we have:

$$-\mathcal{L}_{\text{mass}}^d = \frac{v_1}{\sqrt{2}} \bar{d}_R^0 \, \mathbf{h_d} \left(\mathbf{1} + \boldsymbol{\Delta}_d^{\phi_1}\right) d_L^0 + \frac{v_2}{\sqrt{2}} \bar{d}_R^0 \, \mathbf{h_d} \, \boldsymbol{\Delta}_d^{\phi_2} \, d_L^0 + \text{H.c.} \equiv \frac{v_1}{\sqrt{2}} \bar{d}_R^0 \, \mathbf{h_d} \left(\mathbf{1} + \boldsymbol{\Delta}_d\right) d_L^0 + \text{h.c.} \quad (9)$$

where $\boldsymbol{\Delta}_d = \boldsymbol{\Delta}_d^{\phi_1} + (v_2/v_1) \, \boldsymbol{\Delta}_d^{\phi_2}$ contains the loop corrections. Transforming the states to the mass basis:

$$d_R^0 = \mathcal{U}_R^d \, d_R \, ; \qquad\qquad d_L^0 = \mathcal{U}_L^d \, d_L = \mathcal{U}_L^Q \, \mathbf{V} \, d_L \, ; \qquad\qquad (10)$$

$$u_R^0 = \mathcal{U}_R^u \, u_R \, ; \qquad\qquad u_L^0 = \mathcal{U}_L^u \, u_L = \mathcal{U}_L^Q \, u_L \, , \qquad\qquad (11)$$

---

[1] In the presence of CP phases, limits from electric dipole moments (EDMs) should also be considered. However, in our scenario we have decoupled sfermions, and heavy Higgs masses are above the TeV. In these conditions, the main contributions to EDMs are due to scalar-pseudoscalar Higgs mixing from the two-loop Barr-Zee diagrams with H_1. As shown in [40, 41], the relevant constraint on our couplings would be, $|\eta_1| \lesssim (0.1 \tan\beta)^2$ which does not playing any relevant role in most of the considered parameter space.

we have:

$$-\mathcal{L}^d_{\text{mass}} = \bar{d}_R \, \widehat{\mathbf{M}}_d \, d_L + \text{h.c.} \qquad \text{with} \quad \widehat{\mathbf{M}}_d = \frac{v_1}{\sqrt{2}} \left(\mathcal{U}^d_R\right)^\dagger \mathbf{h_d} \, [\mathbf{1} + \boldsymbol{\Delta}_d] \, \mathcal{U}^Q_L \, \mathbf{V} \tag{12}$$

where $\widehat{\mathbf{M}}_d = \text{diag}\,(m_d, m_s, m_b)$ is the physical diagonal mass matrix for the down-type quarks. Using the flavour basis where $\mathcal{U}^Q_L = \mathcal{U}^u_R = \mathcal{U}^d_R = \mathbf{1}$ and introducing $\mathbf{R}_d = \mathbf{1} + \boldsymbol{\Delta}_d$, we can relate the physical masses to the Yukawa couplings through the following expression:

$$\mathbf{h_d} = \frac{\sqrt{2}}{v_1} \widehat{\mathbf{M}}_d \, \mathbf{V}^\dagger \, \mathbf{R}^{-1}_d \,. \tag{13}$$

Using this expression in Eq. (8), we obtain the FC effective Lagrangian for the interactions of the physical neutral Higgses with the down-type quarks [55, 56]:

$$\mathcal{L}_{\text{FC}} = -\frac{g}{2M_W} \left[H_i \, \bar{d} \left(\widehat{\mathbf{M}}_d \, \mathbf{g}^L_{H_i \bar{d}d} \, P_L \, + \, \mathbf{g}^R_{H_i \bar{d}d} \, \widehat{\mathbf{M}}_d \, P_R \right) d \right]. \tag{14}$$

A simplified expression for the Higgs couplings can be obtained working in the single-Higgs-insertion (SHI) approximation [55] where:

$$\boldsymbol{\Delta}^{\phi_1}_d = \boldsymbol{\Delta}^{a_1}_d = \mathbf{F}^0_d;$$

$$\boldsymbol{\Delta}^{\phi_2}_d = \boldsymbol{\Delta}^{a_2}_d = \mathbf{G}^0_d : \tag{15}$$

$$\boldsymbol{\Delta}_d = \mathbf{F}^0_d + \tfrac{v_2}{v_1}\mathbf{G}^0_d = \mathbf{F}^0_d + \tan\beta \, \mathbf{G}^0_d \tag{16}$$

For large $\tan\beta$ values, the $\mathbf{F}^0_d$ term can be neglected and therefore $\mathbf{R}_d$ may be approximated as:

$$\mathbf{R}_d = \mathbf{1} + \tan\beta \, \mathbf{G}^0_d. \tag{17}$$

Then the Higgs couplings in the Lagrangian of Eq. (14) will be simplified to:

$$\mathbf{g}^L_{H_i \bar{d}d} = \frac{\mathcal{O}_{1i}}{\cos\beta} \mathbf{V}^\dagger \mathbf{R}^{-1}_d \mathbf{V} + \frac{\mathcal{O}_{2i}}{\cos\beta} \mathbf{V}^\dagger \mathbf{R}^{-1}_d \mathbf{G}^0_d \mathbf{V} + i\mathcal{O}_{3i} \tan\beta \left[\frac{1}{\sin^2\beta} \mathbf{V}^\dagger \mathbf{R}^{-1}_d \mathbf{V} - \frac{1}{\tan^2\beta} \right], \tag{18}$$

$$\mathbf{g}^R_{H_i \bar{d}d} = \left(\mathbf{g}^L_{H_i \bar{d}d} \right)^\dagger . \tag{19}$$

By noting $\mathbf{V}^\dagger \mathbf{R}^{-1}_d \mathbf{G}^0_d \mathbf{V} = \left(\mathbf{1} - \mathbf{V}^\dagger \mathbf{R}^{-1}_d \mathbf{V}\right) / \tan\beta$, we observe that the size of flavour violation is dictated by the off-diagonal components of the matrix $\mathbf{V}^\dagger \mathbf{R}^{-1}_d \mathbf{V} = \mathbf{V}^\dagger \left(\mathbf{1} + \tan\beta \, \mathbf{G}^0_d\right)^{-1} \mathbf{V}$. Therefore the Higgs couplings to the down-type quarks will be determined once $\mathbf{G}^0_d$ is known.

The detailed expression for this quantity $\mathbf{G}^0_d$ in terms of soft SUSY-breaking parameters can be found in Appendix A. Observe that in this formalism, flavour violation from off-diagonal components of the sfermion mass matrices as well as its diagonal parts has been included.

B. FC Higgs decays

For the computation of the decay width $\Gamma(H_i \rightarrow \bar{b}s + \bar{s}b)$, we consider the relevant terms involving b and s quarks in Eq. (14). Introducing the effective couplings $y_{L_i} \equiv m_b \mathbf{g}^L_{H_i \bar{b}s}/v$ and $y_{R_i} \equiv m_s \mathbf{g}^R_{H_i \bar{b}s}/v$, we may write:

$$\mathcal{L}_{H_i bs} = -H_i \bar{b} \Big[y_{L_i} P_L + y_{R_i} P_R \Big] s + \text{H.c.} \tag{20}$$

This expression can be rewritten as:

$$\mathcal{L}_{H_i bs} = -H_i \bar{b} \Big[g_i^S + i g_i^P \gamma_5 \Big] s + \text{H.c.} \tag{21}$$

with $g_i^S = (y_{L_i} + y_{R_i})/2$ and $g_i^P = i(y_{L_i} - y_{R_i})/2$. Then, using Eq. (28) of [57], the decay width can be obtained as:

$$\Gamma\left(H_i \rightarrow \bar{b}s + \bar{s}b\right) = 2 \times \frac{N_c\, m_{H_i}}{16\pi} \lambda^{1/2}\left(1, x_b, x_s\right) \kappa_{QCD} \times$$
$$\Big[(1 - x_b - x_s)\left(|y_{L_i}|^2 + |y_{R_i}|^2\right) - 4\sqrt{x_b x_s}\, \Re e\left(y_{L_i} y_{R_i}^*\right) \Big] \tag{22}$$

where $\kappa_{QCD} = 1 + 5.67\, \alpha_S\left(m_{H_i}^2\right)/\pi$ including the QCD correction, $x_f = m_f^2/m_{H_i}^2$ and $\lambda\left(1, a, b\right) = (1 - a - b)^2 - 4ab$. Note that in y_{L_i, R_i} the masses involved are $m_{b,s} = m_{b,s}\left(m_{H_i}\right)$.

III. EXPERIMENTAL CONSTRAINTS

In our analyses, we use two main sets of experimental data: collider constraints on Higgs and supersymmetric particles and constraints on flavour changing processes. Collider constraints come mainly from CMS and ATLAS, the two general purpose experiments in the LHC that claimed the observation of a new 125 GeV particle in 2012 [1, 2]. Regarding indirect processes, we use the current flavour experimental data associated with B-meson decays and mass differences.

A. Collider Constraints

ATLAS and CMS are the two general purpose LHC experiments which provide the most accurate data concerning the Higgs boson and SUSY. In particular, we will consider the Higgs $\gamma\gamma$ signal, the $\tau\tau$-channel limits, and direct limits on supersymmetric particle masses. All these constraints have been already used in previous works [58, 59], so we refer to them for details. Here, we will summarize the basic requirements taken into account during the analysis. First, according to the experimental data so far, we require a diphoton signal in the range:

$$0.75 \leq \mu_{\gamma\gamma}^{LHC} \leq 1.55 \,, \tag{23}$$

where μ_X is the signal strength for a Higgs decaying to X: $\mu_X = [\sigma(pp \to H) \times \mathrm{BR}(H \to X)]/[\sigma(pp \to H)_{\mathrm{SM}} \times \mathrm{BR}(H \to X)_{\mathrm{SM}}]$.

On the other hand, we apply the limits set by CMS [60] and ATLAS [61] in the $H \to \tau\tau$-channel. Specifically, we use the 95 % Confidence Level (CL) limits on the gluon-fusion and b-associated Higgs boson production cross sections times the branching ratio into τ pairs, presented in Fig. 4 in Ref. [60] and Fig. 11 in Ref. [61]. In these analysis, extended searches for extra Higgs states have been carried out for masses up to 1 TeV at 95% CL. In our case, these limits will be imposed to all three neutral Higgs states: H_1, H_2 and H_3.

Finally, we must take into account direct bounds on SUSY masses. Taking into account that the effects of SUSY particles on Higgs couplings are non-decoupling, we can apply conservative limits on the masses. For the gluino, we set the mass limit at $m_{\tilde{g}} \gtrsim 1.4$ TeV when the neutralino mass is below ~ 700 GeV, in agreement with the exclusion limits from ATLAS [62] and CMS [63]. The mass limits for the third generation squarks are taken from ATLAS data [62] as: $m_{\tilde{t}_1} \gtrsim 650$ GeV when the neutralino mass is below 250 GeV, or $m_{\tilde{t}_1} - m_{\chi_1^0} \lesssim 175$ GeV when it is nearly degenerate with the LSP. Finally, according to ATLAS searches [62], the chargin mass limits are: $m_{\tilde{\chi}_1^\pm} \gtrsim 700$ GeV for dominant decays into charged leptons, or $m_{\chi_1^\pm} \gtrsim 450$ GeV when the decays into weak bosons prevail.

B. FC Constraints

Apart from these data coming from the collider experiments, there is another kind of processes that can play a significant part in the search for SM extensions. As presented in the previous works [58, 59], flavour constraints may be a powerful weapon to restrict the parameter space, especially the parameter $\tan\beta$, even in the absence of complex flavour structures beyond the SM Yukawa couplings. Therefore, for our analysis, we will make use of indirect bounds coming from B-meson decays and mass differences. In particular, we will consider: $B_s^0 \to \mu^+\mu^-$, ΔM_{B_s} and $B \to X_s\gamma$. In the case of the rare decay $B_s^0 \to \mu^+\mu^-$, the latest experimental value for its branching fraction is the combined analysis of CMS and LHCb data at 7 TeV and 8 TeV, with integrated luminosities of 25 fb^{-1} and 3 fb^{-1} respectively [64]:

$$\mathrm{BR}\left(B_s^0 \to \mu^+\mu^-\right) = \left(2.8_{-0.6}^{+0.7}\right) \cdot 10^{-9} \tag{24}$$

Hence, our analysis bound at 2σ will be:

$$\mathrm{BR}\left(B_s^0 \to \mu^+\mu^-\right) \leq 4.2 \cdot 10^{-9} \tag{25}$$

Another valuable flavour decay is $B \to X_s\gamma$, which becomes the most restrictive constraint for medium and low $\tan\beta$ values. Combining the BaBar, Belle and CLEO analysis, the world average value given by HFAG [65] is:

$$\mathrm{BR}\left(B \to X_s\gamma\right) = (3.43 \pm 0.21 \pm 0.07) \cdot 10^{-4} \tag{26}$$

For the opposite $\tan\beta$ regime, that is large $\tan\beta$ values, the main experimental result turns out to be the $\mathrm{B_s}$-meson mass difference ΔM_{B_s}. The present experimental value is [65]:

$$\Delta M_{B_s} = (17.757 \pm 0.021) \quad \mathrm{ps}^{-1} \tag{27}$$

We will require in our analysis:

$$15.94\,\mathrm{ps}^{-1} \leq \Delta M_{B_s} \leq 19.83\,\mathrm{ps}^{-1} \tag{28}$$

where we included the theoretical error on $f_{B_s}\sqrt{B_s} = 262 \pm 10$ [66].

IV. NUMERICAL ANALYSIS

Before we present the results of our numerical analysis, we present first some approximate analytic expressions for $\mathbf{G}_d^0$, $\mathbf{R}_d^{-1}$ and, finally, $\left(\mathbf{V}^\dagger\mathbf{R}_d^{-1}\mathbf{V}\right)_{32,23}$, which are most relevant to the FC Higgs decay into b and s quarks. Note that the FC structure is common to the two situations under consideration: the full MSSM framework and the generic Supersymmetric SM.

From Eq. (18) and using $\mathbf{V}^\dagger\mathbf{R}_d^{-1}\mathbf{G}_d^0\mathbf{V} = \left(\mathbf{1} - \mathbf{V}^\dagger\mathbf{R}_d^{-1}\mathbf{V}\right)/\tan\beta$, we observe that the size of flavour violation is dictated by the off-diagonal components of the matrix $\mathbf{V}^\dagger\mathbf{R}_d^{-1}\mathbf{V}$ which can be determined once $\mathbf{G}_d^0$ is known.

As shown in Appendix A, one may need the explicit forms of the flavour violating matrices $\delta\widetilde{\mathbf{M}}^2_{Q,U,D}$ and $\delta\mathbf{a}_u$ to derive $\mathbf{G}_d^0$. Assuming universality for the first two generations, we introduce the following flavour parametrization [2]

$$\widetilde{\mathbf{M}}^2_X = \begin{pmatrix} \rho & 0 & 0 \\ 0 & \rho & \delta_X \\ 0 & \delta_X & 1 \end{pmatrix} \widetilde{M}^2_{X_3}, \qquad \mathbf{h}_u^{-1}\mathbf{a}_u = \begin{pmatrix} \rho & 0 & 0 \\ 0 & \rho & \delta_{A_u} \\ 0 & \delta_{A_u} & 1 \end{pmatrix} A_{u_3} \tag{29}$$

---

[2] We are assuming, for simplicity, symmetric Yukawa and trilinear matrices at tree-level. In general, $\left(\mathbf{h}_u^{-1}\mathbf{a}_u\right)_{23}$ and $\left(\mathbf{h}_u^{-1}\mathbf{a}_u\right)_{32}$ can be different from each other and complex.

where $X = Q, U, D$ and then $\delta\widetilde{\mathbf{M}}^2_{Q,U,D}$ and $\delta\mathbf{a}_u$ are given by

$$\delta\widetilde{\mathbf{M}}^2_{Q,U,D} = \widetilde{\mathbf{M}}^2_{Q,U,D} - \widetilde{M}^2_{Q,U,D}\mathbf{1}\,, \qquad\qquad \delta\mathbf{a}_u = \mathbf{a}_u - \mathbf{h}_u A_u \qquad (30)$$

with $\widetilde{M}^2_{Q,U,D} = \frac{1}{3}\mathrm{Tr}\left(\widetilde{\mathbf{M}}^2_{Q,U,D}\right) = \frac{1}{3}\left(2\rho + 1\right)\widetilde{M}^2_{Q_3,U_3,D_3}$ and $A_u = \frac{1}{3}\mathrm{Tr}\left(\mathbf{h}_u^{-1}\mathbf{a}_u\right) = \frac{1}{3}\left(2\rho + 1\right)A_{u_3}$. In the basis where the up-type Yukawa quarks are diagonal $\mathbf{h}_u = \mathrm{diag}\left(y_u, y_c, y_t\right)$, we have,

$$\delta\widetilde{\mathbf{M}}^2_X = \begin{pmatrix} \frac{\rho-1}{3} & 0 & 0 \\ 0 & \frac{\rho-1}{3} & \delta_X \\ 0 & \delta_X & -\frac{2}{3}\left(\rho-1\right) \end{pmatrix}\widetilde{M}^2_{X_3}\,, \qquad \delta\mathbf{a}_u = \begin{pmatrix} \frac{\rho-1}{3}\,y_u & 0 & 0 \\ 0 & \frac{\rho-1}{3}\,y_c & \delta_{A_u}\,y_c \\ 0 & \delta_{A_u}\,y_t & -\frac{2}{3}\left(\rho-1\right)y_t \end{pmatrix}A_{u_3}\,. \quad (31)$$

Inserting the above expression for $\delta\widetilde{\mathbf{M}}^2_{Q,U,D}$ and $\delta\mathbf{a}_u$ into Eqs. (A2) and (A3), we obtain

$$\mathbf{G}^0_d \simeq \begin{pmatrix} \epsilon & 0 & 0 \\ 0 & \epsilon & \delta\epsilon_{23} \\ 0 & \delta\epsilon_{32} & \epsilon + \eta \end{pmatrix} \qquad (32)$$

where ϵ, η, $\delta\epsilon_{32}$ and $\delta\epsilon_{23}$ are parameters containing the main loop contributions of Eq. (A2) and Eq. (A3). Here, it is worth mentioning that EW corrections in those two equations have been neglected, while the down-type Yukawa couplings have been approximated as $\mathbf{h}_d \simeq \frac{\sqrt{2}}{v_1}\widehat{\mathbf{M}}_d\mathbf{V}^\dagger$. The explicit forms of the diagonal entries ϵ and η are given in Appendix A, while the off-diagonal elements, which are the key ones for us as will be seen later, are given by the following expressions:

$$\delta\epsilon_{23} = \delta_L\left[\frac{2\alpha_s}{3\pi}\mu^* M_3^* \tilde{M}^2_{Q_3} K\left(\tilde{M}^2_Q, \tilde{M}^2_D, |M_3|^2\right) + \frac{|y_t|^2}{16\pi^2}\mu^* A_t^* \tilde{M}^2_{Q_3} K\left(\tilde{M}^2_Q, \tilde{M}^2_D, |\mu|^2\right)\right] \qquad (33)$$

$$+ \delta_{A_u}\left[\frac{|y_t|^2}{16\,\pi^2}\mu^* A_t^* I\left(\tilde{M}^2_Q, \tilde{M}^2_U, |\mu|^2\right)\right] + \delta_R\left[\frac{2\alpha_s}{3\pi}\frac{V_{33}^* y_b}{V_{22}^* y_s}\mu^* M_3^* \tilde{M}^2_{D_3} K\left(\tilde{M}^2_D, \tilde{M}^2_Q, |M_3|^2\right)\right]$$

$$+ (\rho-1)\left[\frac{2\alpha_s}{3\pi}\frac{V_{32}^*}{V_{22}^*}\mu^* M_3^* \tilde{M}^2_{D_3} K\left(\tilde{M}^2_D, \tilde{M}^2_Q, |M_3|^2\right)\right]$$

$$\delta\epsilon_{32} = \delta_L\left[\frac{2\alpha_s}{3\pi}\mu^* M_3^* \tilde{M}^2_{Q_3} K\left(\tilde{M}^2_Q, \tilde{M}^2_D, |M_3|^2\right)\right] + \delta_{A_u}\left[\frac{|y_c|^2}{16\pi^2}\mu^* A_t^* I\left(\tilde{M}^2_Q, \tilde{M}^2_U, |\mu|^2\right)\right] \qquad (34)$$

$$+ \delta_R\left[\frac{2\alpha_s}{3\pi}\left(\frac{V_{22}^* y_s}{V_{33}^* y_b} - \frac{V_{23}^{*2} y_b}{V_{22}^* V_{33}^* y_s}\right)\mu^* M_3^* \tilde{M}^2_{D_3} K\left(\tilde{M}^2_D, \tilde{M}^2_Q, |M_3|^2\right)\right]$$

$$- (\rho-1)\left[\frac{2\alpha_s}{3\pi}\frac{V_{23}^*}{V_{33}^*}\mu^* M_3^* \tilde{M}^2_{D_3} K\left(\tilde{M}^2_D, \tilde{M}^2_Q, |M_3|^2\right)\right]$$

where $\delta_Q \equiv \delta_L$ and $\delta_U = \delta_D \equiv \delta_R$. We note that there are four types of flavour-violating terms

proportional to δ_L, δ_{A_u}, δ_R, and $(\rho - 1)$ [3]. Then, we obtain

$$
\mathbf{R}_d^{-1} \simeq \begin{pmatrix} \frac{(1+\epsilon \tan \beta)(1+(\epsilon+\eta) \tan \beta)-\delta\epsilon_{23}\delta\epsilon_{32} \tan^2 \beta}{\text{Det}(\mathbf{R}_d)} & 0 & 0 \\ 0 & \frac{(1+\epsilon \tan \beta)(1+(\epsilon+\eta) \tan \beta)}{\text{Det}(\mathbf{R}_d)} & -\frac{\delta\epsilon_{23}(1+\epsilon \tan \beta) \tan \beta}{\text{Det}(\mathbf{R}_d)} \\ 0 & -\frac{\delta\epsilon_{32}(1+\epsilon \tan \beta) \tan \beta}{\text{Det}(\mathbf{R}_d)} & \frac{(1+\epsilon \tan \beta)^2}{\text{Det}(\mathbf{R}_d)} \end{pmatrix} \quad (35)
$$

from

$$
\mathbf{R}_d = \mathbf{1} + \tan \beta \, \mathbf{G}_d^0 \simeq \begin{pmatrix} 1 + \epsilon \tan \beta & 0 & 0 \\ 0 & 1 + \epsilon \tan \beta & \delta\epsilon_{23} \tan \beta \\ 0 & \delta\epsilon_{32} \tan \beta & 1 + (\epsilon + \eta) \tan \beta \end{pmatrix}. \quad (36)
$$

As we will see, the most relevant flavour-violating matrix element in the FC Higgs decay $H_i \to bs$

is $\left(\mathbf{V}^\dagger \mathbf{R}_\mathbf{d}^{-1} \mathbf{V} \right)_{32,23}$. In principle, this matrix element $\left(\mathbf{V}^\dagger \mathbf{R}_\mathbf{d}^{-1} \mathbf{V} \right)_{32}$ is:

$$
\left(\mathbf{V}^\dagger \mathbf{R}_d^{-1} \mathbf{V} \right)_{32} = \sum_{i,j=1}^{3} \mathbf{V}_{i3}^* \left(\mathbf{R}_d^{-1} \right)_{ij} \mathbf{V}_{j2}
$$

$$
= \sum_{i=1}^{3} \left[\mathbf{V}_{i3}^* \left(\mathbf{R}_d^{-1} \right)_{ii} \mathbf{V}_{i2} \right] + \mathbf{V}_{23}^* \left(\mathbf{R}_d^{-1} \right)_{23} \mathbf{V}_{32} + \mathbf{V}_{33}^* \left(\mathbf{R}_d^{-1} \right)_{32} \mathbf{V}_{22}. \quad (37)
$$

Using Eq. (35) for $\mathbf{R}_d^{-1}$ and taking into account the unitarity of the CKM matrix, we can write:

$$
\sum_{i=1}^{3} \left[\mathbf{V}_{i3}^* \left(\mathbf{R}_d^{-1} \right)_{ii} \mathbf{V}_{i2} \right] = (\mathbf{V}_{13}^* \mathbf{V}_{12} + \mathbf{V}_{23}^* \mathbf{V}_{22}) \frac{(1 + \epsilon \tan \beta) \eta \tan \beta}{\text{Det} (\mathbf{R}_d)} - \mathbf{V}_{13}^* \mathbf{V}_{12} \frac{\delta\epsilon_{23}\delta\epsilon_{32} \tan^2 \beta}{\text{Det} (\mathbf{R}_d)}. \tag{38}
$$

In this expression, we can neglect all the terms proportional to $\mathbf{V}_{13}^* \mathbf{V}_{12} \sim 8 \times 10^{-4}$ with respect to $\mathbf{V}_{23}^* \mathbf{V}_{22} \sim 4 \times 10^{-2}$, even for the last term proportional to $\delta\epsilon_{23}\delta\epsilon_{32}$, which, as can be seen from Eqs. (33,34) and (A6,A7), is, for sizeable mass insertion (MI), of the same order as $\epsilon \times \eta$.

Then, in Eq. (37), if we have similar values of the off-diagonal elements $\left(\mathbf{R}_d^{-1} \right)_{23}$ and $\left(\mathbf{R}_d^{-1} \right)_{32}$, the former can also be neglected with respect to later, being suppressed by an additional $|\mathbf{V}_{23}^* \mathbf{V}_{32}| \sim 2.10^{-3}$. Therefore, in the presence of sizeable mass insertions $\delta_{L,R} \geq \mathbf{V}_{23}^* \mathbf{V}_{22}$, we have $\delta\epsilon_{32} \geq \eta \times \mathbf{V}_{23}^* \mathbf{V}_{22}$ and then we can safely take,

$$
\left(\mathbf{V}^\dagger \mathbf{R}_\mathbf{d}^{-1} \mathbf{V} \right)_{32} \simeq \mathbf{V}_{33}^* \mathbf{V}_{22} \left(\mathbf{R}_\mathbf{d}^{-1} \right)_{32} + \mathbf{V}_{23}^* \mathbf{V}_{22} \frac{(1 + \epsilon \tan \beta) \eta \tan \beta}{\text{Det} (\mathbf{R}_d)} \simeq \left(\mathbf{R}_\mathbf{d}^{-1} \right)_{32}. \quad (39)
$$

Repeating the same exercise with $\left(\mathbf{V}^\dagger \mathbf{R}_\mathbf{d}^{-1} \mathbf{V} \right)_{23}$, we obtain,

$$
\left(\mathbf{V}^\dagger \mathbf{R}_\mathbf{d}^{-1} \mathbf{V} \right)_{23} \simeq \mathbf{V}_{22}^* \mathbf{V}_{33} \left(\mathbf{R}_\mathbf{d}^{-1} \right)_{23} + \mathbf{V}_{22}^* \mathbf{V}_{23} \frac{(1 + \epsilon \tan \beta) \eta \tan \beta}{\text{Det} (\mathbf{R}_d)} \simeq \left(\mathbf{R}_\mathbf{d}^{-1} \right)_{23}. \quad (40)
$$

---

[3] Please note that our definition of δ_{A_u} in Eq (31) makes it different from the δ_{LR} usually defined in the literature.

The study of these matrix elements is very interesting because of their dependence on δ_L, δ_R and δ_{A_u}. Looking at Eq. (34) for $\delta\epsilon_{32}$ and comparing the δ_L and δ_R contributions, we can see that the δ_R term is suppressed by the difference $\left(y_s/y_b - \mathbf{V}_{23}^{*}{}^2 y_b/y_s\right) \simeq -0.013$ with respect to the δ_L term. Therefore, these matrix elements, and especially $\left(\mathbf{R}_d^{-1}\right)_{32}$, will have very different values for these two mass insertions. Also from these equations, it is evident that, if $\delta_L \simeq \delta_{A_u}$, we would obtain similar results from both types of mass insertions to $\delta\epsilon_{23}$, but its contributions to $\delta\epsilon_{32}$ would be suppressed by an additional factor $(y_c/y_t)^2$. In any case, the δ_{A_u} contributions to $\delta\epsilon_{23}$ and $\delta\epsilon_{32}$ are always smaller than the δ_R contributions. For this reason, we will only consider the cases of the δ_L and δ_R insertions

All the results of the numerical analysis presented in the following sections and the corresponding figures are done with the `CPsuperH2.3` code [57, 67, 68].

A. Full MSSM framework

In the full MSSM framework, the effective FC Higgs couplings are given by:

$$y_{L_i} \equiv \frac{m_b}{v} \mathbf{g}_{H_i\bar{b}s}^L = \frac{m_b}{v}\left(\frac{\mathcal{O}_{1i}}{\cos\beta} - \frac{\mathcal{O}_{2i}}{\sin\beta} + i\tan\beta\frac{\mathcal{O}_{3i}}{\sin^2\beta}\right)\left(\mathbf{V}^\dagger \mathbf{R}_d^{-1}\mathbf{V}\right)_{32}, \tag{41}$$

$$y_{R_i} \equiv \frac{m_s}{v} \mathbf{g}_{H_i\bar{b}s}^R = \frac{m_s}{v}\left(\frac{\mathcal{O}_{1i}}{\cos\beta} - \frac{\mathcal{O}_{2i}}{\sin\beta} - i\tan\beta\frac{\mathcal{O}_{3i}}{\sin^2\beta}\right)\left(\mathbf{V}^\dagger \mathbf{R}_d^{-1}\mathbf{V}\right)_{23}^{*}, \tag{42}$$

and the decay width, Eq. (22), is:

$$\begin{aligned}
\Gamma\left(H_i \to \bar{b}s + \bar{s}b\right) &\simeq \frac{3m_{H_i}}{8\pi}\kappa_{QCD}\left(|y_{L_i}|^2 + |y_{R_i}|^2\right) \\
&\simeq \frac{3m_{H_i}m_b^2}{8\pi v^2}\kappa_{QCD}\left[\left(\frac{\mathcal{O}_{1i}}{\cos\beta} - \frac{\mathcal{O}_{2i}}{\sin\beta}\right)^2 + \left(\tan\beta\frac{\mathcal{O}_{3i}}{\sin^2\beta}\right)^2\right] \\
&\quad \times \left(\left|\left(\mathbf{V}^\dagger \mathbf{R}_d^{-1}\mathbf{V}\right)_{32}\right|^2 + \frac{m_s^2}{m_b^2}\left|\left(\mathbf{V}^\dagger \mathbf{R}_d^{-1}\mathbf{V}\right)_{23}\right|^2\right),
\end{aligned} \tag{43}$$

In the case of δ_L insertions, from the discussion in the previous section, we observe $|y_{R_i}| \ll |y_{L_i}|$ due to the m_s/m_b suppression with $\left(\mathbf{V}^\dagger \mathbf{R}_d^{-1}\mathbf{V}\right)_{32} \sim \left(\mathbf{V}^\dagger \mathbf{R}_d^{-1}\mathbf{V}\right)_{23}^{*}$. In the presence of δ_R insertions the situation is more involved and both terms must be considered.

Now, considering the total decay widths of the Higgs bosons, we will obtain the corresponding branching ratios. In the case of the lightest Higgs, its total decay width is dominated by the decay into two b-quarks, two W-bosons and two τ-leptons. Thus:

$$\Gamma_{H_1} = \frac{m_{H_1}m_b^2}{8\pi v^2}\left[\left(3\kappa_{QCD} + \frac{m_\tau^2}{m_b^2}\right)\tan^2\beta\left(\mathcal{O}_{11}^2 + \mathcal{O}_{31}^2\right) + I_{PS}\frac{m_{H_1}^2}{m_b^2}\left(\mathcal{O}_{21} + \frac{\mathcal{O}_{11}}{\tan\beta}\right)^2\right] \tag{44}$$

where in the large-$\tan\beta$ limit we have used $(\mathcal{O}_{11}^2/\cos^2\beta + \tan^2\beta\,\mathcal{O}_{31}^2) \simeq \tan^2\beta\,(\mathcal{O}_{11}^2 + \mathcal{O}_{31}^2)$ and $(\sin\beta\,\mathcal{O}_{21} + \cos\beta\,\mathcal{O}_{11})^2 \simeq (\mathcal{O}_{21} + \mathcal{O}_{11}/\tan\beta)^2$. I_{PS} in the second term refers to the phase-space integral in the Higgs decay into two W bosons [57] and can be approximated by $I_{PS} \simeq 6.7 \times 10^{-4}$ when $m_{H_1} = 125$ GeV. Then, the branching ratio will be:

$$\text{BR}\left(H_1 \to \bar{b}s + \bar{s}b\right) = \left|(\mathbf{V}^\dagger\mathbf{R}_d^{-1}\mathbf{V})_{32}\right|^2 \frac{3\,\kappa_{QCD}\left[\left(\frac{\mathcal{O}_{11}}{\cos\beta} - \frac{\mathcal{O}_{21}}{\sin\beta}\right)^2 + \left(\frac{\mathcal{O}_{31}}{\sin\beta\cos\beta}\right)^2\right]}{\left(3\,\kappa_{QCD} + \frac{m_\tau^2}{m_b^2}\right)\tan^2\beta\,(\mathcal{O}_{11}^2 + \mathcal{O}_{31}^2) + I_{PS}\frac{m_{H_1}^2}{m_b^2}\left(\mathcal{O}_{21} + \frac{\mathcal{O}_{11}}{\tan\beta}\right)^2} \, . \tag{45}$$

For the heavier Higgses, and for $\tan\beta \gtrsim 30$, the total decay width is dominated by the bottom and tau widths:

$$\Gamma_{H_2} \simeq \frac{m_{H_2}m_b^2}{8\pi v^2}\left(3\,\kappa_{QCD} + \frac{m_\tau^2}{m_b^2}\right)\tan^2\beta\left(\mathcal{O}_{12}^2 + \mathcal{O}_{32}^2\right) \tag{46}$$

using $(\mathcal{O}_{12}^2/\cos^2\beta + \tan^2\beta\,\mathcal{O}_{32}^2) \simeq \tan^2\beta\,(\mathcal{O}_{12}^2 + \mathcal{O}_{32}^2)$ and the branching ratio is:

$$\text{BR}\left(H_2 \to \bar{b}s + \bar{s}b\right) = 3\,\kappa_{QCD}\left|\left(\mathbf{V}^\dagger\mathbf{R}_d^{-1}\mathbf{V}\right)_{32}\right|^2 \frac{\left(\frac{\mathcal{O}_{12}}{\cos\beta} - \frac{\mathcal{O}_{22}}{\sin\beta}\right)^2 + \left(\frac{\mathcal{O}_{32}}{\sin\beta\cos\beta}\right)^2}{\left(3\,\kappa_{QCD} + \frac{m_\tau^2}{m_b^2}\right)\tan^2\beta\,(\mathcal{O}_{12}^2 + \mathcal{O}_{32}^2)} \, . \tag{47}$$

In a previous work [59], we showed that the latest LHC data for the Higgs signal in the diphoton channel strongly constrains the Higgs mixing within a general CP-violating model. In particular, if we consider the lightest Higgs as the recently discovered boson at 126 GeV, its mixing conditions are $(\mathcal{O}_{11}^2 + \mathcal{O}_{31}^2) \sim 1/\tan^2\beta$ and $\mathcal{O}_{21}^2 \sim 1$. Additionally, using the parametrization presented in Eq. (4), we have:

$$\text{BR}\left(H_1 \to \bar{b}s + \bar{s}b\right) = \left|\left(\mathbf{V}^\dagger\mathbf{R_d^{-1}}\mathbf{V}\right)_{32}\right|^2 \frac{3\,\kappa_{QCD}\,(\delta_1^2 + \eta_1^2)}{\left(3\,\kappa_{QCD} + \frac{m_\tau^2}{m_b^2}\right) + I_{PS}\frac{m_{H_1}^2}{m_b^2}} \, . \tag{48}$$

Still following [59], it was also showed that the diphoton condition establishes for the heavier Higgs mixings that: $(\mathcal{O}_{1i}^2 + \mathcal{O}_{3i}^2) \sim 1$ and $\mathcal{O}_{2i} \lesssim 1/\tan\beta$, $i = 2, 3$. Hence:

$$\text{BR}\left(H_2 \to \bar{b}s + \bar{s}b\right) \simeq \left|\left(\mathbf{V}^\dagger\mathbf{R_d^{-1}}\mathbf{V}\right)_{32}\right|^2 \frac{3\,\kappa_{QCD}}{3\,\kappa_{QCD} + \frac{m_\tau^2}{m_b^2}} \tag{49}$$

where we have considered $\tan\beta \geq 3$ and, therefore, $1/\cos\beta \simeq \tan\beta$ and $\sin\beta \simeq 1$ in a good approximation.

1. Left-handed (L) insertion

First, we analyze the case with $\delta_L \neq 0$ and $\delta_R = 0$:

$$\delta\epsilon_{32(L)} \simeq \delta_L\,\frac{2\alpha_s}{3\pi}\,\mu^*\,M_3^*\,\tilde{M}_{Q_3}^2\,K\left(\tilde{M}_Q^2, \tilde{M}_D^2, |M_3|^2\right) \sim -3\cdot 10^{-3}\delta_L \tag{50}$$
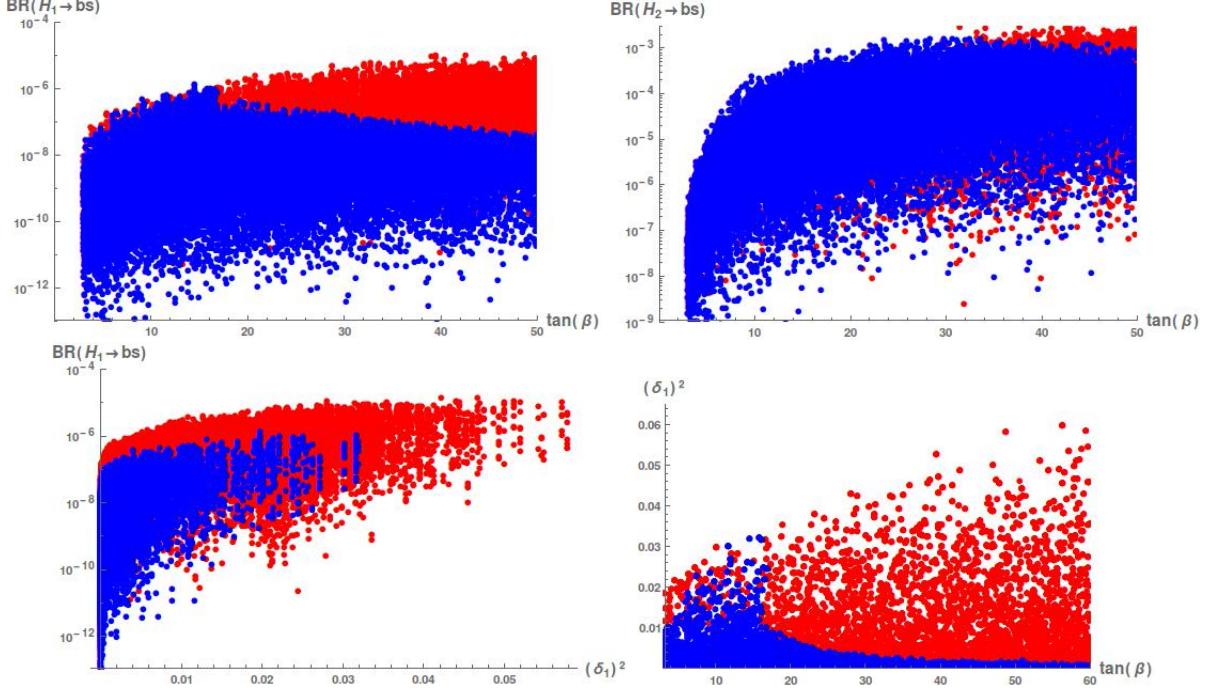
FIG. 1: A full MSSM framework with LL insertion with $\delta_L \neq 0$ and $\delta_{A_u} = \delta_R = 0$: The upper frames show the dependence of the estimated branching ratios for $H_{1,2} \to \bar{b}s + \bar{s}b$ on $\tan\beta$. The lower-left frame is for the dependence of $B(H_1 \to bs)$ on δ_1^2 and the lower-right frame for the δ_1^2 dependence on $\tan\beta$. Blue (dark) points satisfy all the constraints considered, while red (light) points violate one or several of these constraints.

where we can see that $\delta\epsilon_{32(L)}$ has a non-decoupling behaviour as it depends only on ratios of sparticle masses and we have used $\tilde{M}_{Q,D,Q_3} \sim 5$ TeV, $M_3 \sim 7$ TeV and $\mu \sim 6$ TeV. Consequently, for the maximum values of $\tan\beta$ and δ_L considered during the scan, $\delta_L \sim 0.5$ [4] and $\tan\beta \sim 60$, we would obtain:

$$\left(\mathbf{R_d^{-1}}\right)^{\max}_{32(L)} \simeq -\frac{\delta\epsilon_{32(L)}\left(1 + \epsilon\tan\beta\right)\tan\beta}{\mathrm{Det}\left(\mathbf{R_d}\right)} \sim \frac{3\cdot 10^{-3} \times 1.5 \times 60}{4} \sim 0.03 \qquad (51)$$

where ϵ, Eq. (A6), and $\mathrm{Det}(\mathbf{R_d})$ for the masses specified above take the values $\epsilon \simeq 0.01$ and $\mathrm{Det}(\mathbf{R}_d) \simeq 4.7$. Therefore:

$$\mathrm{BR}\left(H_1 \to \bar{b}s + \bar{s}b\right)^{\max}_{(L)} \simeq \left|\left(\mathbf{V}^\dagger\mathbf{R_d^{-1}}\mathbf{V}\right)_{32(L)}\right|^2 \frac{3\,\kappa_{QCD} \times (\delta_1^2 + \eta_1^2)}{\left(3\,\kappa_{QCD} + \frac{m_\tau^2}{m_b^2}\right) + I_{PS}\frac{126^2}{m_b^2}} \sim 5\cdot 10^{-4}\,(\delta_1^2 + \eta_1^2) \quad (52)$$

$$\mathrm{BR}\left(H_2 \to \bar{b}s + \bar{s}b\right)^{\max}_{(L)} \simeq \left|\left(\mathbf{V}^\dagger\mathbf{R_d^{-1}}\mathbf{V}\right)_{32(L)}\right|^2 \frac{3\,\kappa_{QCD}}{3\,\kappa_{QCD} + \frac{m_\tau^2}{m_b^2}} \sim 10^{-3} \qquad (53)$$

_____

[4] Notice that, effectively, there is no bound from low-energy FC processes on this MI for such heavy gluinos and squarks.

Fig. 1 shows the results of our scans. Blue points are those which satisfy the whole set of constraints while red points are excluded because of the violation of one or more of them. In the upper frames of Fig. 1, we represent the branching ratios for H_1 and H_2 versus $\tan\beta$ (for all considerations, H_3 will be equivalent to H_2 given that they are nearly degenerated for the range of masses considered here). As can be seen in these two plots, before applying the low-energy constraints, the branching ratio grows with $\tan\beta$ (red points). However, the final result is very different from this when we impose experimental limits from B-mesons (blue points). Whereas for heavy Higgses few points become excluded, in the case of the lightest Higgs the effect is more notable. Indeed, looking at the upper-left frame of Fig. 1 we can say that the tendency is completely opposite and the branching ratio decreases for $\tan\beta > 20$.

This behaviour is mainly due to the $B_s^0 \to \mu^+\mu^-$ constraint. This branching ratio is given in Eq. (B13) with C_S, Eq. (B15), and C_P, Eq. (B16), containing the SUSY contributions. The dominant contributions come from the heavy Higgses and we have:

$$C_{S,P} \propto 2\frac{\tan^2\beta}{m_{H_j}^2}\left(\mathbf{V}^\dagger\mathbf{R}_d^{-1}\mathbf{V}\right)_{32}^*\left[\left(\mathcal{O}_{1j} - \frac{\mathcal{O}_{2j}}{\tan^2\beta}\right)^2 + \mathcal{O}_{3j}^2\right] \sim 2\frac{\tan^2\beta}{m_{H_j}^2}\left(\mathbf{R}_d^{-1}\right)_{32}^* \qquad (54)$$

with $j = 2, 3$. This dependence on $\tan^3\beta$ (the matrix element $\left(\mathbf{R}_d^{-1}\right)_{32}^*$ carries an additional $\tan\beta$) and the heavy Higgs masses explains why this decay provides such a restrictive constraint for relatively small m_{H_2,H_3}^2 and medium-to-large values of $\tan\beta$.

In fact, $\mathrm{BR}(H_1 \to bs)$ is suppressed at medium and large $\tan\beta$ values while $\mathrm{BR}(H_2 \to bs)$ is not. This is due to fact that $\mathrm{BR}(H_1 \to bs)$ is proportional to δ_1 and η_1, which in the MSSM are of order $v^2/M_{H_2}^2$. Then, B-meson constraints are more restrictive for light m_{H_2} which also correspond to the largest $\mathrm{BR}(H_1 \to bs)$. On the other hand $\mathrm{BR}(H_2 \to bs)$ is independent of δ_1 or η_1 and the H_2 mass. The B-meson constraints are not effective here if m_{H_2} is large enough and therefore we can reach large branching ratios for large $\tan\beta$ values. Furthermore, this branching ratio saturates for medium-to-large values of $\tan\beta$ when both the FC decay width and the total decay width have the same $\tan\beta$ dependence.

Moreover, the lower-left frame of Fig. 1 shows the branching ratio for H_1 versus δ_1^2. As seen in Eq. (52), for $\delta_1^2 \gtrsim 0.02$ the branching ratio is of the order 10^{-5}. However, the implementation of B-meson constraints here reduces this value by more than one order of magnitude.

Finally, in the lower-right frame of Fig. 1, we present the δ_1^2 dependence on $\tan\beta$. We observe that, before imposing B-meson constraints, larger values of (δ_1^2) are possible when $\tan\beta$ grows.
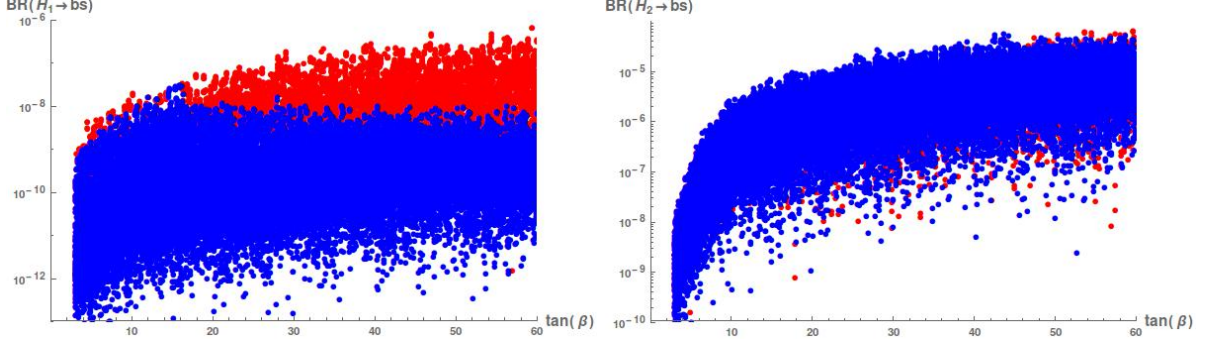
FIG. 2: A full MSSM framework with RR insertion with $\delta_R \neq 0$ and $\delta_{A_u} = \delta_L = 0$: The left frame shows the dependence of $\mathrm{BR}(H_1 \to bs)$ on $\tan\beta$ and the right frame shows the dependence of $\mathrm{BR}(H_2 \to bs)$ on $\tan\beta$. Again, blue (dark) points satisfy all the constraints considered, while red (light) points violate one or several of these constraints.

However, B-meson constraints become very effective for $\tan\beta \gtrsim 17$ as shown by the blue points in this plot. This could be understood by noting that the Higgs contributions to the $\Delta B = 1$ and $\Delta B = 2$ processes are inversely proportional to the heavy Higgs mass squared. Therefore, to suppress these processes for large $\tan\beta$, large Higgs masses are required. Accordingly, we expect smaller $|\delta_1|$ as $\tan\beta$ grows since, as we have seen, $|\delta_1| \propto v^2/m_{H_2}^2$ in the MSSM.

2. Right-handed (R) insertion

Now we consider the case, $\delta_R \neq 0$ and $\delta_L = \delta_{A_u} = 0$, we have from Eqs. (34) and (50):

$$\delta\epsilon_{32(R)} \simeq \delta_R \left(\frac{\mathbf{V}_{22}^* \, y_s}{\mathbf{V}_{33}^* \, y_b} - \frac{\mathbf{V}_{23}^{*\,2} \, y_b}{\mathbf{V}_{22}^* \, \mathbf{V}_{33}^* \, y_s} \right) \frac{\delta\epsilon_{32(L)}}{\delta_L} \sim 0.013 \times 3 \times 10^{-3} \, \delta_R \sim 5 \cdot 10^{-5} \, \delta_R \,, \quad (55)$$

$$\left(\mathbf{R}_d^{-1} \right)_{32(R)} \simeq \left(\frac{\mathbf{V}_{22}^* \, y_s}{\mathbf{V}_{33}^* \, y_b} - \frac{\mathbf{V}_{23}^{*\,2} \, y_b}{\mathbf{V}_{22}^* \, \mathbf{V}_{33}^* \, y_s} \right) \left(\mathbf{R}_d^{-1} \right)_{32(L)} \sim 4 \cdot 10^{-4} \, \delta_R \,. \quad (56)$$

In this case, the value of the off-diagonal element $(\mathbf{R}_d^{-1})_{32}$ is of the order of 10^{-4} and this implies that the contributions $\mathbf{V}_{23}^* \mathbf{V}_{22}$ in Eq. (38) and $\left(\mathbf{R}_d^{-1} \right)_{23}$ in Eq. (37) or y_{R_i} in Eq. (42), can be important. Thus:

$$\left(\mathbf{V}^\dagger \mathbf{R}_d^{-1} \mathbf{V} \right)_{32(R)}^{\max} \simeq \left(\mathbf{R}_d^{-1} \right)_{32(R)} + 2 \cdot 10^{-3} \left(\mathbf{R}_d^{-1} \right)_{23(R)} + 0.04 \, \frac{(1 + \epsilon \tan\beta) \, \eta \, \tan\beta}{\mathrm{Det} \, (\mathbf{R}_d)}$$

$$\sim -4 \cdot 10^{-4} \delta_R - 2 \cdot 10^{-3} \, \frac{\delta\epsilon_{23(R)} \times 1.5 \times 60}{4} + 0.04 \, \frac{1.5 \times 4 \cdot 10^{-3} \times 60}{4} \quad (57)$$

where we used the same values for the parameters as in Eq. (51) and $\delta\epsilon_{23(R)}$ is now enhanced by a factor y_b/y_s:

$$\delta\epsilon_{23(R)} \sim \delta_R \frac{2\alpha_s}{3\pi} \frac{y_b}{y_s} \mu^* M_3^* \tilde{M}_{D_3}^2 K\left(\tilde{M}_Q^2, \tilde{M}_D^2, |M_3|^2\right) \sim -0.1\,\delta_R\,. \tag{58}$$

Therefore, we obtain,

$$\left(\mathbf{V}^\dagger \mathbf{R}_d^{-1} \mathbf{V}\right)_{32(R)}^{\max} \sim 4(\delta_R + 1) \cdot 10^{-3} \tag{59}$$

Thus, for $\delta_R = 0.5$, the branching ratios are:

$$\mathrm{BR}\left(H_1 \to \bar{b}s + \bar{s}b\right)_{(R)}^{\max} \simeq \left|\left(\mathbf{V}^\dagger \mathbf{R}_d^{-1} \mathbf{V}\right)_{32(R)}\right|^2 \frac{3\,\kappa_{QCD}(\delta_1^2 + \eta_1^2)}{\left(3\,\kappa_{QCD} + \frac{m_\tau^2}{m_b^2}\right) + I_{PS}\frac{126^2}{m_b^2}} \sim 1.5 \cdot 10^{-5}\,(\delta_1^2 + \eta_1^2) \tag{60}$$

$$\mathrm{BR}\left(H_2 \to \bar{b}s + \bar{s}b\right)_{(R)}^{\max} \simeq \left|\left(\mathbf{V}^\dagger \mathbf{R}_d^{-1} \mathbf{V}\right)_{32(R)}\right|^2 \frac{3\,\kappa_{QCD}}{3\,\kappa_{QCD} + \frac{m_\tau^2}{m_b^2}} \sim 2 \cdot 10^{-5} \tag{61}$$

The results of our scans for this case are shown in Fig. 2. As before, these results are in agreement with the numerical values if B-meson constraints are not taken into account. Once they are incorporated into the analysis, the lightest Higgs branching ratio is reduced by more than one order of magnitude. Also, taking into account, from Eq. (57), that both the MI and MI-independent contributions are of the same order only for large δ_R, the BR is completely independent of δ_R.

B. Generic supersymmetric SM

After computing these branching ratios in the MSSM framework, we now perform our analysis in a generic supersymmetric model. Therefore, we present here a model-independent analysis, meaning that, in fact, we consider a generic Higgs mixing matrix with possible additional Higgs states. In this case, we have $\mathcal{O}_{11}^2 + \mathcal{O}_{21}^2 + \mathcal{O}_{31}^2 \leq 1$ and the parameters δ_1 and/or η_1 entering $\Gamma(H_1 \to \bar{b}s + \bar{s}b)$ can be sizeable.

The expressions for the decay widths and branching ratios, Eqs. (43–49), are still valid in the generic supersymmetric scenario. The main difference now is that the parameters δ_1 and η_1 are only constrained by experimental results on Higgs decays and low-energy FCNC processes. Notice, however, that the flavour-changing entries in $\mathbf{R_d^{-1}}$ do not change in the two models.

In Fig. 3, we show the FC branching ratios of H_1 and H_2 for $\delta_L \neq 0$ and $\delta_{A_u} = \delta_R = 0$ in the generic supersymmetric SM. These figures can be compared with Fig. 1 which shows the corresponding branching ratios in the MSSM framework.
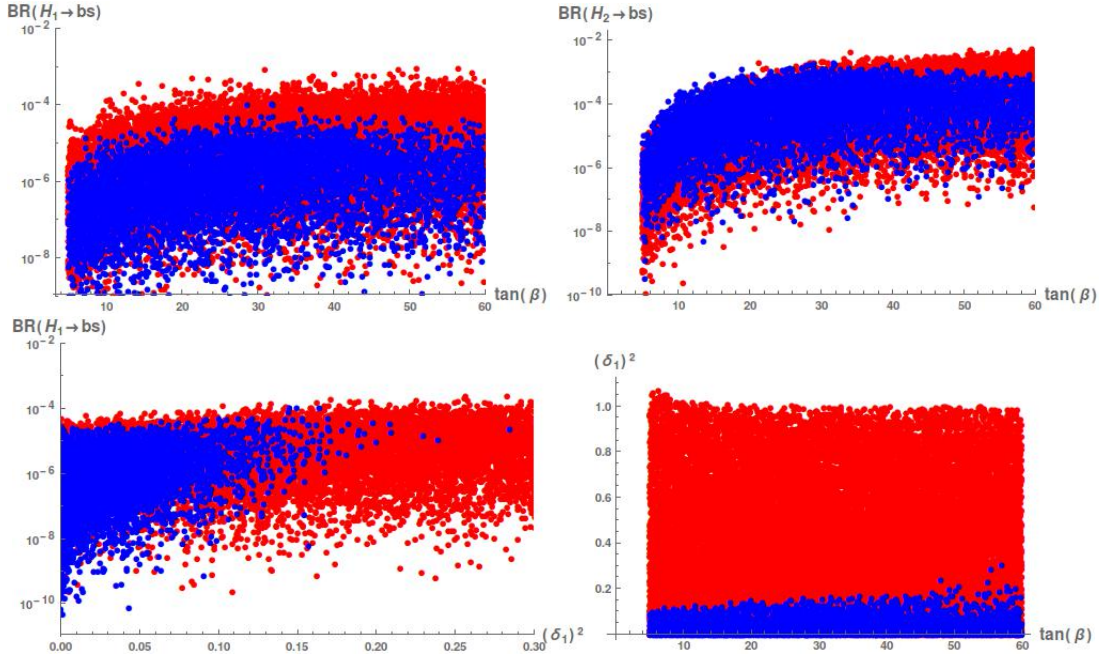
FIG. 3: A generic supersymmetric SM with L insertion with $\delta_L \neq 0$ and $\delta_{A_u} = \delta_R = 0$: The upper frames show the dependence of the estimated branching ratios for $H_{1,2} \to \bar{b}s + \bar{s}b$ on $\tan\beta$. The lower-left frame is for the dependence of $B(H_1 \to bs)$ on δ_1^2 and the lower-right frame for the δ_1^2 dependence on $\tan\beta$. Blue (dark) points satisfy all the constraints considered, while red (light) points violate one or several of these constraints.

In the MSSM framework, the mixing angles are obtained through a minimization of the scalar potential and both δ_1 and η_1 are of the order of $v^2/m_{H_2}^2$ from the diagonalization of the neutral Higgs mass matrix. In the generic supersymmetric scenario we treat δ_1 and η_1 as free parameters that do not depend a priori on the ratio $v^2/m_{H_2}^2$, but are only constrained by the different experimentally measured Higgs branching ratios and B-meson constraints. This is why $\mathrm{BR}(H_1 \to bs)$ in Fig 1 is two orders of magnitude smaller that the largest possible value in Figure 3. The different distribution of the points allowed by B-meson constraints is due to the same reason. In the MSSM scenario, Higgs flavour changing processes are mediated by the heavy Higgses and therefore are only important for light m_{H_2} which, as we have seen, correspond also to the largest δ_1 and η_1 and therefore to the largest branching ratios. In the generic supersymmetric SM, it is, in principle, possible to have a large δ_1 with a heavy H_2 and therefore the B-meson constraints are not so efficient.

On the other hand, the FC decays of the heavy Higgses $H_{2,3}$ are independent of the values of δ_1 and η_1 as can be seen in Eq. (49). Therefore, the upper-right frames of Figs. 1 and 3 are very similar and we obtain very similar results for $\mathrm{BR}(H_2 \to bs)$ in the MSSM framework and in the generic supersymmetric SM.

Also, as shown in the lower-right plot in Fig. 3, the allowed values of $(\delta_1)^2$ are completely independent of $\tan\beta$ as the B-meson constraints, which depending on $(\tan\beta)^n/m_{H_2}^4$ can always be satisfied by adjusting conveniently the value of m_{H_2}. In this case, the upper limit for $(\delta_1)^2$ is fixed by the $H_1 \to \gamma\gamma$ decay which as shown in [59], requires $(\mathcal{O}_{11}^2 + \mathcal{O}_{31}^2) \sim 1/\tan^2\beta$ and $\mathcal{O}_{21}^2 \sim 1 - 1/\tan^2\beta$. Using the definition of δ_1 and in the limit $\mathcal{O}_{31} \ll 1$, with the above constraints, $(\delta_1)^2 \lesssim 0.17$ for $\tan\beta \gtrsim 10$, as we see numerically in this plot.

In summary, the main difference in the generic supersymmetric SM is that $\mathrm{BR}(H_1 \to bs)$ could reach a value of $\sim 10^{-4}$ consistently with present experimental constraints. This value is still too small to be observed in the large background of a hadron collider, but it could be tested in a leptonic linear collider in the near future.

V. CONCLUSIONS

In this paper, we have analyzed the FC Higgs decay $H_i \to bs$ for the different Higgs states in both an MSSM scenario and a more general supersymmetric SM framework. The importance of this observable is that effects of heavy particles do not decouple and may provide a first sign of new physics for heavy supersymmetric masses beyond collider reach. Before we carried out our numerical analysis, we derived approximated analytic expressions for the off-diagonal entries of $\left(\mathbf{V}^\dagger \mathbf{R}_d^{-1} \mathbf{V}\right)$ which dictate the size of flavour violation. In an MSSM framework we showed that, even in the presence of large off-diagonal flavour entries in the sfermion mass matrices, for the light Higgs, $\mathrm{BR}(H_1 \to bs) \lesssim 10^{-6}$ consistently with present experimental constraints, while for heavy Higgs states $\mathrm{BR}(H_{2,3} \to bs)$ can still be $\sim 10^{-3}$. In a more general supersymmetric scenario, where we allowed for non-minimal Higgs mixings, the branching ratio $\mathrm{BR}(H_1 \to bs)$ can reach values $\sim \mathcal{O}(10^{-4})$, while $\mathrm{BR}(H_{2,3} \to bs)$ remain of the order of $\sim 10^{-3}$. We find that the results of the numerical analysis are well in accord with the estimations made using the approximated analytic expression for $\left(\mathbf{V}^\dagger \mathbf{R}_d^{-1} \mathbf{V}\right)$. Although these small branching ratios are clearly out of reach for the LHC due to the very large b-quark background, a full study in a linear collider environment could still be worth pursuing.

Appendix A: FC Higgs couplings

In this appendix, we present the explicit expression for $\mathbf{G}_d^0$ associated with the FCNC Higgs couplings in Eq. (14),

$$\mathbf{G}_d^0 = \langle \mathbf{\Delta}_d^{\Phi_2} + \delta\mathbf{\Delta}_d^{\Phi_2} \rangle_0 \tag{A1}$$

$$\begin{aligned}
\langle \mathbf{\Delta}_d^{\Phi_2} \rangle_0 = {} & \mathbf{1}\,\frac{2\alpha_3}{3\pi}\mu^* M_3^* I\left(\widetilde{M}_Q^2, \widetilde{M}_D^2, |M_3|^2\right) - \mathbf{1}\,\frac{\alpha_1}{36\pi}\mu^* M_1^* I\left(\widetilde{M}_Q^2, \widetilde{M}_D^2, |M_1|^2\right) \\
& + \frac{\mathbf{h}_u^\dagger \mathbf{h}_u}{16\pi^2}\mu^* A_u^* I\left(\widetilde{M}_Q^2, \widetilde{M}_U^2, |\mu|^2\right) - \frac{3\alpha_2}{8\pi}\mu^* M_2^* I\left(\widetilde{M}_Q^2, \widetilde{M}_D^2, |\mu|^2\right) \\
& - \mathbf{1}\,\frac{\alpha_1}{24\pi}\mu^* M_1^* I\left(\widetilde{M}_Q^2, |M_1|^2, |\mu|^2\right) - \mathbf{1}\,\frac{\alpha_1}{12\pi}\mu^* M_1^* I\left(\widetilde{M}_D^2, |M_1|^2, |\mu|^2\right)
\end{aligned} \tag{A2}$$

$$\begin{aligned}
\langle \delta\mathbf{\Delta}_d^{\Phi_2} \rangle_0 = {} & \frac{2\alpha_3}{3\pi}\mu^* M_3^* \left[\delta\widetilde{\mathbf{M}}_Q^2 K\left(\widetilde{M}_Q^2, \widetilde{M}_D^2, |M_3|^2\right) + \mathbf{h}_d^{-1}\delta\widetilde{\mathbf{M}}_D^2 \mathbf{h}_d K\left(\widetilde{M}_D^2, \widetilde{M}_Q^2, |M_3|^2\right)\right] \\
& - \frac{\alpha_1}{36\pi}\mu^* M_1^* \left[\delta\widetilde{\mathbf{M}}_Q^2 K\left(\widetilde{M}_Q^2, \widetilde{M}_D^2, |M_1|^2\right) + \mathbf{h}_d^{-1}\delta\widetilde{\mathbf{M}}_D^2 \mathbf{h}_d K\left(\widetilde{M}_D^2, \widetilde{M}_Q^2, |M_1|^2\right)\right] \\
& + \frac{1}{16\pi^2}\mu^* A_u^* \left[\mathbf{h}_u^\dagger\delta\widetilde{\mathbf{M}}_U^2 \mathbf{h}_u K\left(\widetilde{M}_U^2, \widetilde{M}_Q^2, |\mu|^2\right) + \delta\widetilde{\mathbf{M}}_Q^2 \mathbf{h}_u^\dagger\mathbf{h}_u K\left(\widetilde{M}_Q^2, \widetilde{M}_U^2, |\mu|^2\right)\right] \\
& + \frac{\delta\mathbf{a}_u^\dagger\mathbf{h}_u}{16\pi^2}\mu^* I\left(\widetilde{M}_Q^2, \widetilde{M}_U^2, |\mu|^2\right) - \frac{3\alpha_2}{8\pi}\mu^* M_2^* \delta\widetilde{\mathbf{M}}_Q^2 K\left(\widetilde{M}_Q^2, \left|\widetilde{M}_2\right|^2, |\mu|^2\right) \\
& - \frac{\alpha_1}{24\pi}\mu^* M_1^*\delta\widetilde{\mathbf{M}}_Q^2 K\left(\widetilde{M}_Q^2, |M_1|^2, |\mu|^2\right) - \frac{\alpha_1}{12\pi}\mu^* M_1^*\mathbf{h}_d^{-1}\delta\widetilde{\mathbf{M}}_D^2 \mathbf{h}_d K\left(\widetilde{M}_D^2, |M_1|^2, |\mu|^2\right)
\end{aligned} \tag{A3}$$

where the loops functions are given by:

$$I(a, b, c) = \frac{ab\ln(a/b) + bc\ln(b/c) + ac\ln(c/a)}{(a-b)(b-c)(a-c)} \tag{A4}$$

$$K(a, b, c) = \frac{\mathrm{d}}{\mathrm{d}a}\left[I(a, b, c)\right] = \frac{b\ln(a/b) + c\ln(c/a)}{(a-b)(b-c)(a-c)} + \frac{(b+c-2a)\,I(a, b, c) + 1}{(a-b)(a-c)} \tag{A5}$$

From here, the elements ϵ, δ, used in the $\mathbf{G}_d^0$ matrix in Eq. (32) are,

$$\epsilon = \frac{2\alpha_s}{3\pi}\mu^* M_3^* I\left(\tilde{M}_Q^2, \tilde{M}_D^2, |M_3|^2\right) + \frac{\rho-1}{3}\left[\frac{2\alpha_s}{3\pi}\mu^* M_3^* \left(\tilde{M}_{D_3}^2 + \tilde{M}_{Q_3}^2\right) K\left(\tilde{M}_Q^2, \tilde{M}_D^2, |M_3|^2\right)\right] \tag{A6}$$

$$\eta = \frac{|y_t|^2}{16\pi^2}\,\mu^* A_u^*\, I\left(\tilde{M}_Q^2, \tilde{M}_U^2, |\mu|^2\right) - \delta_R\left[\frac{2\alpha_s}{3\pi}\,\mu^*\, M_3^*\,\frac{V_{23}^*}{V_{33}^*}\tilde{M}_{D_3}^2\, K\left(\tilde{M}_Q^2, \tilde{M}_D^2, |M_3|^2\right)\right] \tag{A7}$$

$$+ (1-\rho)\left[\frac{2}{3}\frac{|y_t|^2}{16\pi^2}\,\mu^*\left(A_t^*\, I\left(\tilde{M}_Q^2, \tilde{M}_U^2, |\mu|^2\right) + A_u^*\left(\tilde{M}_{U_3}^2 + \tilde{M}_{Q_3}^2\right) K\left(\tilde{M}_Q^2, \tilde{M}_U^2, |\mu|^2\right)\right)\right.$$

$$\left. + \frac{2\alpha_s}{3\pi}\,\mu^*\, M_3^*\left(\tilde{M}_{D_3}^2 + \tilde{M}_{Q_3}^2\right) K\left(\tilde{M}_Q^2, \tilde{M}_D^2, |M_3|^2\right)\right]$$

Appendix B: B-physics constraints

The main FC processes associated with B-Mesons that we consider in our analysis are ΔM_{B_s} and $\bar{B}_s^0 \to \mu^+\mu^-$, although other constraints like $\mathrm{BR}(B \to X_s\gamma)$ are also included.

In the case of ΔM_{B_s}, we use the expression in [55], given by:

$$\Delta M_{B_s} = 2\left|\left\langle \bar{B}_s^0|H_{eff}^{\Delta B=2}|B_s^0\right\rangle_{SM} + \left\langle \bar{B}_s^0|H_{eff}^{\Delta B=2}|B_s^0\right\rangle_{SUSY}\right| \tag{B1}$$

where the SUSY contribution is [55]:

$$\left\langle \bar{B}_s^0|H_{eff}^{\Delta B=2}|B_s^0\right\rangle_{SUSY} = 2310\mathrm{ps}^{-1}\left(\frac{\widehat{B}_{B_s}^{1/2}F_{B_s}}{265\,\mathrm{MeV}}\right)^2\left(\frac{\nu_B}{0.55}\right) \times$$

$$\left[0.88\left(C_2^{LR(DP)} + C_2^{LR(2HDM)}\right) - 0.52\left(C_1^{SLL(DP)} + C_1^{SRR(DP)}\right)\right]. \tag{B2}$$

where the Wilson coefficients above $C_2^{LR(DP)}$, $C_2^{LR(2HDM)}$, $C_1^{SLL(DP)}$ and $C_1^{SRR(DP)}$ are associated with double-penguin and box diagrams.

The Wilson coefficients $C_1^{SLL(DP)}$, $C_1^{SRR(DP)}$, $C_2^{LR(DP)}$ and $C_2^{LR(2HDM)}$ related to the SUSY contribution of the B_s-meson mass difference in Eq. (B2) are,

$$C_1^{SLL(DP)} = -\frac{16\pi^2 m_b^2}{\sqrt{2}G_F M_W^2}\sum_{i=1}^3 \frac{\mathbf{g}_{H_i\bar{b}s}^L \mathbf{g}_{H_i\bar{b}s}^L}{m_{H_i}} \tag{B3}$$

$$C_1^{SRR(DP)} = -\frac{16\pi^2 m_s^2}{\sqrt{2}G_F M_W^2}\sum_{i=1}^3 \frac{\mathbf{g}_{H_i\bar{b}s}^R \mathbf{g}_{H_i\bar{b}s}^R}{m_{H_i}} \tag{B4}$$

$$C_2^{LR(DP)} = -\frac{32\pi^2 m_b m_s}{\sqrt{2}G_F M_W^2}\sum_{i=1}^3 \frac{\mathbf{g}_{H_i\bar{b}s}^L \mathbf{g}_{H_i\bar{b}s}^R}{m_{H_i}} \tag{B5}$$

$$C_2^{LR(2HDM)} = \left.C_2^{LR(2HDM)}\right|_{H^\pm H^\mp} + \left.C_2^{LR(2HDM)}\right|_{W^\pm H^\mp}. \tag{B6}$$

The couplings of the charged Higgses and Goldstone bosons to fermions, Eq. (3.38) of Ref.[56], are given by:

$$\mathcal{L} \supset -\frac{g}{2M_W}\left[H^-\bar{d}\left(\widehat{\mathbf{M}}_d\,\mathbf{g}_{H-}^L\, P_L + \mathbf{g}_{H-}^R\,\widehat{\mathbf{M}}_u\, P_R\right) u + G^-\bar{d}\left(\widehat{\mathbf{M}}_d\,\mathbf{g}_{G-}^L\, P_L + \mathbf{g}_{G-}^R\,\widehat{\mathbf{M}}_u\, P_R\right) u\right] + \mathrm{h.c.} \tag{B7}$$

and in the large $\tan\beta$ limit, we have:

$$\mathbf{g}_{H^-}^L = -\tan\beta\mathbf{V}^\dagger\mathbf{R}_d^{-1} + \mathbf{V}^\dagger\mathbf{R}_d^{-1}\mathbf{G}_d^0 \qquad\qquad \mathbf{g}_{H^-}^R = -\frac{1}{\tan\beta}\mathbf{V}^\dagger \tag{B8}$$

$$\mathbf{g}_{G^-}^L = \mathbf{V}^\dagger \qquad\qquad \mathbf{g}_{G^-}^R = -\mathbf{V}^\dagger \tag{B9}$$

Then $C_2^{LR(2HDM)}$ includes two main contributions: one associated with box diagrams for two $H_l^\pm$ and another for $W^\mp H^\pm$ box diagrams. From Eqs. (4.4) and (4.5) in Ref.[69], we have:

$$C_2^{LR(2HDM)}\Big|_{H^\pm H^\mp} = \frac{8m_b m_s m_t^4}{M_W^2} \sum_{k,l=H,G} \mathbf{g}_{H_l^-\ 33}^L \mathbf{g}_{H_l^-\ 32}^{L\dagger} \mathbf{g}_{H_k^-\ 33}^R \mathbf{g}_{H_k^-\ 32}^{R\dagger} D_0\left(M_{H_l^-}^2, M_{H_k^-}^2, m_t^2, m_t^2\right) \tag{B10}$$

$$C_2^{LR(2HDM)}\Big|_{W^\pm H^\mp} = -8m_b m_s \sum_{i,j=1}^{3} \sum_{k=H,G} \mathbf{g}_{H_k^-\ 3i}^L \mathbf{g}_{H_k^-\ j2}^{L\dagger} \mathbf{V}^\dagger{}_{3j} \mathbf{V}_{i2}\ D_2\left(M_W^2, M_{H_k^-}^2, m_{q_i}^2, m_{q_j}^2\right) \tag{B11}$$

where $D_0(a,b,c,d)$ and $D_2(a,b,c,d)$ are the corresponding loop functions which can be found in Ref.[69]

The decay $\bar{B}_s^0 \to \mu^+\mu^-$ is described by the effective Hamiltonian,

$$H_{\text{eff}}^{\Delta B=1} = -2\sqrt{2}G_F V_{tb}V_{ts}^* \left(C_S\mathcal{O}_S + C_P\mathcal{O}_P + C_{10}\mathcal{O}_{10}\right) \tag{B12}$$

where the relevant operators are $\mathcal{O}_S = \frac{e^2}{16\pi^2}m_b\left(\bar{q}P_R b\right)\left(\bar{\mu}\mu\right)$, $\mathcal{O}_P = \frac{e^2}{16\pi^2}m_b\left(\bar{q}P_R b\right)\left(\bar{\mu}\gamma_5\mu\right)$ and $\mathcal{O}_{10} = \frac{e^2}{16\pi^2}\left(\bar{q}\gamma^\mu P_L b\right)\left(\bar{\mu}\gamma_\mu\gamma_5\mu\right)$.

Neglecting the non-holomorphic vertices on the leptonic sector as well as the contributions proportional to the lighter quark masses $m_{d,s}$, the branching ratio is given by

$$\text{BR}\left(\bar{B}_s^0 \to \mu^+\mu^-\right) = \frac{G_F^2\alpha_{\text{em}}^2}{16\pi^3} M_{B_s}\tau_{B_s}\left|V_{tb}V_{ts}^*\right|^2 \sqrt{1 - \frac{4\,m_\mu^2}{M_{B_s}^2}}\left[\left(1 - \frac{4m_\mu^2}{M_{B_s}^2}\right)|F_S^s|^2 + |F_P^s + 2m_\mu F_A^s|^2\right] \tag{B13}$$

where τ_{B_s} is the total lifetime of the B_s meson and the form factors are:

$$F_{S,P}^s = -\frac{i}{2}M_{B_s}^2 F_{Bs}\frac{m_b}{m_b + m_q}C_{S,P}, \qquad F_A^s = -\frac{i}{2}F_{B_s}C_{10}, \tag{B14}$$

with the Wilson coefficients,

$$C_S = \frac{2\pi m_\mu}{\alpha_{\text{em}}}\frac{1}{V_{tb}V_{ts}^*}\sum_{i=1}^{3}\frac{\mathbf{g}_{H_i\bar{s}b}^R\ g_{H_i\bar{\mu}\mu}^S}{m_{H_i}^2}, \tag{B15}$$

$$C_P = i\frac{2\pi m_\mu}{\alpha_{\text{em}}}\frac{1}{V_{tb}V_{ts}^*}\sum_{i=1}^{3}\frac{\mathbf{g}_{H_i\bar{s}b}^R\ g_{H_i\bar{\mu}\mu}^P}{m_{H_i}^2}, \tag{B16}$$

$$C_{10} = -4.221 \tag{B17}$$

where C_{10} is the leading SM contribution, and $g^S_{H_i\bar{\mu}\mu} = \frac{\mathcal{O}_{1i}}{\cos\beta}$ and $g^P_{H_i\bar{\mu}\mu} = -\tan\beta\,\mathcal{O}_{3i}$ are the Higgs couplings to the charged leptons.

[1] G. Aad *et al.* [ATLAS Collaboration], Phys. Lett. B **716**, 1 (2012) [arXiv:1207.7214 [hep-ex]].

[2] S. Chatrchyan *et al.* [CMS Collaboration], Phys. Lett. B **716**, 30 (2012) [arXiv:1207.7235 [hep-ex]].

[3] G. C. Branco, P. M. Ferreira, L. Lavoura, M. N. Rebelo, M. Sher and J. P. Silva, Phys. Rept. **516**, 1 (2012) [arXiv:1106.0034 [hep-ph]].

[4] H. P. Nilles, Phys. Rept. **110**, 1 (1984).

[5] H. E. Haber and G. L. Kane, Phys. Rept. **117**, 75 (1985).

[6] C. Hamzaoui, M. Pospelov and M. Toharia, Phys. Rev. D **59**, 095005 (1999) [hep-ph/9807350].

[7] S. R. Choudhury and N. Gaur, Phys. Lett. B **451**, 86 (1999) [hep-ph/9810307].

[8] K. S. Babu and C. F. Kolda, Phys. Rev. Lett. **84**, 228 (2000) [hep-ph/9909476].

[9] P. H. Chankowski and L. Slawianowska, Phys. Rev. D **63**, 054012 (2001) [hep-ph/0008046].

[10] G. Isidori and A. Retico, JHEP **0111**, 001 (2001) [hep-ph/0110121].

[11] C. Bobeth, T. Ewerth, F. Kruger and J. Urban, Phys. Rev. D **66**, 074021 (2002) [hep-ph/0204225].

[12] A. J. Buras, P. H. Chankowski, J. Rosiek and L. Slawianowska, Phys. Lett. B **546**, 96 (2002) [hep-ph/0207241].

[13] A. J. Buras, P. H. Chankowski, J. Rosiek and L. Slawianowska, Nucl. Phys. B **659**, 3 (2003) [hep-ph/0210145].

[14] P. Paradisi, JHEP **0602**, 050 (2006) [hep-ph/0508054].

[15] A. Arhrib, D. K. Ghosh, O. C. W. Kong and R. D. Vaidya, Phys. Lett. B **647**, 36 (2007) [hep-ph/0605056].

[16] A. J. Buras, M. V. Carlucci, S. Gori and G. Isidori, JHEP **1010**, 009 (2010) [arXiv:1005.5310 [hep-ph]].

[17] A. Crivellin, Phys. Rev. D **83**, 056001 (2011) [arXiv:1012.4840 [hep-ph]].

[18] A. Crivellin, L. Hofer and J. Rosiek, JHEP **1107**, 017 (2011) [arXiv:1103.4272 [hep-ph]].

[19] A. Crivellin and C. Greub, Phys. Rev. D **87**, 015013 (2013) [Phys. Rev. D **87**, 079901 (2013)] [arXiv:1210.7453 [hep-ph]].

[20] A. Goudelis, O. Lebedev and J. h. Park, Phys. Lett. B **707**, 369 (2012) [arXiv:1111.1715 [hep-ph]].

[21] E. Gabrielli and B. Mele, Phys. Rev. D **83**, 073009 (2011) [arXiv:1102.3361 [hep-ph]].

[22] G. Blankenburg, J. Ellis and G. Isidori, Phys. Lett. B **712**, 386 (2012) [arXiv:1202.5704 [hep-ph]].

[23] M. Arana-Catania, E. Arganda and M. J. Herrero, JHEP **1309**, 160 (2013) [arXiv:1304.3371 [hep-ph]].

[24] W. D. Goldberger, B. Grinstein and W. Skiba, Phys. Rev. Lett. **100**, 111802 (2008) [arXiv:0708.1463 [hep-ph]].

[25] J. Fan, W. D. Goldberger, A. Ross and W. Skiba, Phys. Rev. D **79**, 035017 (2009) [arXiv:0803.2040 [hep-ph]].

[26] S. Casagrande, F. Goertz, U. Haisch, M. Neubert and T. Pfoh, JHEP **0810**, 094 (2008) [arXiv:0807.4937 [hep-ph]].

[27] A. Azatov, M. Toharia and L. Zhu, Phys. Rev. D **80**, 035016 (2009) [arXiv:0906.1990 [hep-ph]].

[28] K. Agashe and R. Contino, Phys. Rev. D **80**, 075016 (2009) [arXiv:0906.1542 [hep-ph]].

[29] J. Fuster *et al.* [DELPHI Collaboration], CERN-OPEN-99-393, CERN-DELPHI-99-81.

[30] G. Eilam, Nucl. Phys. Proc. Suppl. **116**, 306 (2003) [hep-ph/0211458].

[31] D. M. Asner *et al.*, arXiv:1310.0763 [hep-ph].

[32] A. Pilaftsis, Phys. Rev. D **58**, 096010 (1998) [hep-ph/9803297].

[33] A. Pilaftsis, Phys. Lett. B **435**, 88 (1998) [hep-ph/9805373].

[34] D. A. Demir, Phys. Rev. D **60**, 095007 (1999) [hep-ph/9905571].

[35] A. Pilaftsis and C. E. M. Wagner, Nucl. Phys. B **553**, 3 (1999) [hep-ph/9902371].

[36] M. Carena, J. R. Ellis, A. Pilaftsis and C. E. M. Wagner, Nucl. Phys. B **586**, 92 (2000) [hep-ph/0003180].

[37] S. Y. Choi, M. Drees and J. S. Lee, Phys. Lett. B **481**, 57 (2000) [hep-ph/0002287].

[38] M. Carena, J. R. Ellis, A. Pilaftsis and C. E. M. Wagner, Nucl. Phys. B **625**, 345 (2002) [hep-ph/0111245].

[39] The ATLAS collaboration [ATLAS Collaboration], ATLAS-CONF-2014-009, ATLAS-CONF-2014-013.

[40] K. Cheung, J. S. Lee, E. Senaha and P. Y. Tseng, JHEP **1406**, 149 (2014) [arXiv:1403.4775 [hep-ph]].

[41] S. Inoue, M. J. Ramsey-Musolf and Y. Zhang, Phys. Rev. D **89**, no. 11, 115023 (2014) [arXiv:1403.4257 [hep-ph]].

[42] T. Banks, Nucl. Phys. B **303**, 172 (1988).

[43] R. Hempfling, Phys. Rev. D **49**, 6168 (1994).

[44] L. J. Hall, R. Rattazzi and U. Sarid, Phys. Rev. D **50**, 7048 (1994) [hep-ph/9306309, hep-ph/9306309].

[45] T. Blazek, S. Raby and S. Pokorski, Phys. Rev. D **52**, 4151 (1995) [hep-ph/9504364].

[46] M. Carena, M. Olechowski, S. Pokorski and C. E. M. Wagner, Nucl. Phys. B **426**, 269 (1994) [hep-ph/9402253].

[47] D. M. Pierce, J. A. Bagger, K. T. Matchev and R. j. Zhang, Nucl. Phys. B **491**, 3 (1997) [hep-ph/9606211].

[48] K. S. Babu and C. F. Kolda, Phys. Lett. B **451**, 77 (1999) [hep-ph/9811308].

[49] F. Borzumati, G. R. Farrar, N. Polonsky and S. D. Thomas, Nucl. Phys. B **555**, 53 (1999) [hep-ph/9902443].

[50] F. Borzumati, G. R. Farrar, N. Polonsky and S. D. Thomas, In *Trieste 1997, Phenomenological aspects of superstring theories* 159-167 [hep-ph/9805314].

[51] H. Eberl, K. Hidaka, S. Kraml, W. Majerotto and Y. Yamada, Phys. Rev. D **62**, 055006 (2000) [hep-ph/9912463].

[52] H. E. Haber, M. J. Herrero, H. E. Logan, S. Penaranda, S. Rigolin and D. Temes, Phys. Rev. D **63**, 055004 (2001) [hep-ph/0007006].

[53] F. Borzumati, C. Greub and Y. Yamada, hep-ph/0305063.

[54] F. Borzumati, C. Greub and Y. Yamada, Phys. Rev. D **69**, 055005 (2004) [hep-ph/0311151].

[55] J. R. Ellis, J. S. Lee and A. Pilaftsis, Phys. Rev. D **76**, 115011 (2007) [arXiv:0708.2079 [hep-ph]].

[56] J. Ellis, R. N. Hodgkinson, J. S. Lee and A. Pilaftsis, JHEP **1002**, 016 (2010) [arXiv:0911.3611 [hep-ph]].

[57] J. S. Lee, A. Pilaftsis, M. Carena, S. Y. Choi, M. Drees, J. R. Ellis and C. E. M. Wagner, Comput. Phys. Commun. **156**, 283 (2004) [hep-ph/0307377].

[58] G. Barenboim, C. Bosch, M. L. L??pez-Iba??ez and O. Vives, JHEP **1311**, 051 (2013) [arXiv:1307.5973 [hep-ph]].

[59] G. Barenboim, C. Bosch, M. L. L??pez-Ib????ez and O. Vives, Phys. Rev. D **90**, no. 1, 015003 (2014) [arXiv:1311.7321 [hep-ph]].

[60] CMS Collaboration [CMS Collaboration], CMS-PAS-HIG-13-021.

[61] G. Aad *et al.* [ATLAS Collaboration], JHEP **1411**, 056 (2014) [arXiv:1409.6064 [hep-ex]].

[62] [ATLAS Collaboration], (2014),
http://atlas.web.cern.ch/Atlas/GROUPS/PHYSICS/CombinedSummaryPlots/SUSY/

[63] [CMS Collaboration], (2014),
https://twiki.cern.ch/twiki/bin/view/CMSPublic/SUSYSMSSummaryPlots8TeV

[64] V. Khachatryan *et al.* [CMS and LHCb Collaborations], Nature **522**, 68 (2015) [arXiv:1411.4413 [hep-ex]].

[65] Y. Amhis *et al.* [Heavy Flavor Averaging Group (HFAG) Collaboration], arXiv:1412.7515 [hep-ex].

[66] S. Aoki *et al.*, Eur. Phys. J. C **74**, 2890 (2014) [arXiv:1310.8555 [hep-lat]].

[67] J. S. Lee, M. Carena, J. Ellis, A. Pilaftsis and C. E. M. Wagner, Comput. Phys. Commun. **180**, 312 (2009) [arXiv:0712.2360 [hep-ph]].

[68] J. S. Lee, M. Carena, J. Ellis, A. Pilaftsis and C. E. M. Wagner, Comput. Phys. Commun. **184**, 1220 (2013) [arXiv:1208.2212 [hep-ph]].

[69] A. J. Buras, P. H. Chankowski, J. Rosiek and L. Slawianowska, Nucl. Phys. B **619**, 434 (2001) [hep-ph/0107048].